Quaternary Science Reviews 87 (2014) 114–134

Contents lists available at ScienceDirect

Quaternary Science Reviews

journal homepage: www.elsevier.com/locate/quascirev

Late Quaternary alluvial fans at the eastern end of the San Bernardino Mountains, Southern California

Lewis A. Owen [a,*], Samuel J. Clemmens [b], Robert C. Finkel [c], Harrison Gray [a]

[a] Department of Geology, University of Cincinnati, Cincinnati, OH 45221, USA
[b] Science Department, Welsh Government, Rhodfa Padarn, Llanbadarn Fawr, Aberystwyth, Ceredigion SY23 3UR, UK
[c] Department of Earth and Planetary Sciences, University of California, Berkeley, CA 94720, USA

ARTICLE INFO

Article history:
Received 24 October 2013
Received in revised form
3 January 2014
Accepted 4 January 2014
Available online 5 February 2014

Keywords:
Alluvial fans
Be-10 terrestrial cosmogenic dating
American Southwest
Sedimentation
Erosion
Climate change

ABSTRACT

Alluvial fans at the eastern end of the San Bernardino Mountains in Southern California provide a record of climate modulated sediment transfer and erosion, and are deformed and displaced in places by active faults. Alluvial fans within two study areas, the Mission Creek and the Whitewater River drainages, were examined using geomorphic, sedimentological, and ^{10}Be terrestrial cosmogenic nuclide (TCN) surface exposure methods to define the timing of alluvial fan formation and erosion, and to examine the role of climatic, tectonic and autocyclic processes. These alluvial fan complexes were studied because they are amongst the best-preserved successions of alluvial fans in southern California and they are located at the mouths of two of the largest drainages, Whitewater River and Mission Creek, in the San Bernardino Mountains and traverse major faults, the Mission Creek and Banning. The alluvial fans comprise bouldery debris deposits that represent deposition dominated by flash flood and debris flow events. TCN surface exposure dating indicates that abandonment/incision of alluvial fan surfaces date to early in the Last Glacial or more likely the penultimate glacial cycle, to marine isotope stage (MIS) 4, and to the Holocene. The lack of alluvial fan ages during the latter part of the Last Glacial (MIS 2 and 3) suggests that there has been little alluvial fan lobe deposition/incision during that time. This is similar to findings for many other alluvial fans throughout the American Southwest, and supports the view that there is a strong climatic control on alluvial fan formation throughout this region. Furthermore, the oldest alluvial fan surfaces in the Mission Creek region are beheaded by the Whitewater River drainage, showing that the oldest alluvial fans in the Mission Creek region underwent significant capture by the Whitewater River drainage. This shows the autocyclic controls are also important on alluvial fan evolution in this region; but the importance of these processes to alluvial fan development in other regions of the American Southwest needs to be more fully assessed. The alluvial fans in the Mission Creek area traverse the Mission Creek fault, but are not deformed by it, which suggests that there may have been little if any movement along this fault since at least MIS 4. In contrast, alluvial fans in the Whitewater River study are displaced by active faults highlighting the influence of tectonism on alluvial fan development in this region. In addition to illustrating the importance of climatic controls on the development of alluvial fans in the American Southwest, a classic region for alluvial fan studies, this study illustrates the complex mixture of autocyclic and allocyclic factors that force alluvial fan development in tectonically active settings.

1. Introduction

Alluvial fans are one of the most common landforms in mountain front areas in arid and semi-arid regions (Bull, 1977; Beaty, 1990; Reheis et al., 1996). Many researchers have suggested that alluvial fans are highly sensitive to environmental change and that they provide an important archive for environmental conditions, notably climate and hydrology, and tectonics (Lustig, 1965; Beaty, 1970; Rockwell et al., 1985; Harvey, 1990, 1997; Lecce, 1990; Bull, 1991; Ritter et al., 1995; Harvey et al., 1999a,b, 2003; Owen et al., 1997, 2006; McDonald et al., 2003; Quigley et al., 2007; Stokes et al., 2007; Frankel et al., 2007a,b; Arboleya et al., 2008; Spelz et al., 2008; Miller et al., 2010; Hedrick et al., 2013). However, deciphering the potentially strong environmental and tectonic record preserved by alluvial fans has been severely restricted by a lack of adequate chronological control. This is mainly because of the absence of preserved organic matter within arid and semi-arid environments that is needed for the standard method of

* Corresponding author. Fax: +1 513 556 4203.
E-mail address: Lewis.Owen@uc.edu (L.A. Owen).

0277-3791/$ – see front matter
http://dx.doi.org/10.1016/j.quascirev.2014.01.003

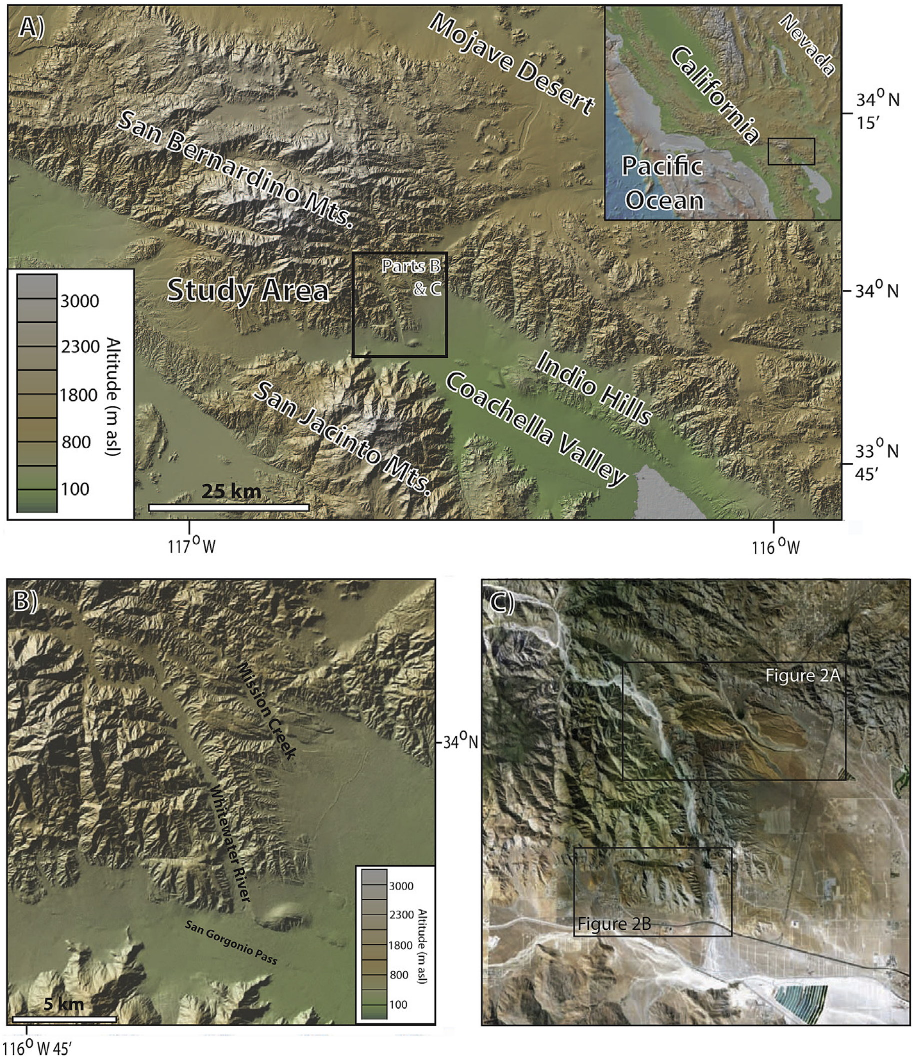

Fig. 1. Digital elevation models for A) regional setting and B) study area produced using GeoMapApp (http://www.geomapapp.org/), and C) Google Earth image of the study area. The inset box on part A) indicates the area shown in parts B) and C).

radiocarbon dating. The development of terrestrial cosmogenic nuclide (TCN) surface exposure, optically stimulated luminescence (OSL) and U-series dating has helped remove this restriction by providing methods to directly determine the timing of alluvial fan formation, erosion and deformation (e.g., Reheis et al., 1996; Zehfuss et al., 2001; Owen et al., 2006, 2011; Frankel et al., 2007a, b; Arboleya et al., 2008; Spelz et al., 2008; Armstrong et al., 2010; Fletcher et al., 2010; Blisniuk et al., 2012). OSL ages provide depositional ages for alluvial fan sediments, whereas TCN ages define the ages of alluvial fan surfaces and therefore represent the timing of abandonment/incision of the surface being dated. U-series dating is usually used to define the ages of carbonate cement formation, which provides minimum ages on landform formation. TCN, OSL, and U-series dating can be used to date alluvial fans beyond the age range for radiocarbon dating (30–50 ka), in some cases to >100 ka.

To examine the nature of alluvial fan development and to help develop a framework for paleoenvironmental and tectonic studies in the American Southwest we examined a succession of alluvial fan surfaces in Whitewater River and Mission Creek drainages at the eastern end of the San Bernardino Mountains along a stretch of the San Andreas Fault system (Fig. 1). We utilize ^{10}Be TCN exposure dating of surface boulders and depth profiles combined with geomorphic and sedimentological analysis to investigate these surfaces.

The Whitewater River and Mission Creek drainages are located at the western end of the Salton Trough in Southern California and they are the primary catchments draining the eastern end of the San Bernardino Mountains within the Transverse Ranges of southern California (Fig. 1). The drainages traverse the Mission Creek and Banning faults, which are two potentially active strands of the San Andreas fault system (Yule et al., 2001; Orozco and Yule, 2003; Orozco, 2004; Yule, 2009; Yule and Spotila, 2010; McGill et al., 2013). Furthermore, the Whitewater River and Mission Creek drainages flow from formerly glaciated source areas within the San Bernardino Mountains and hence alluvial fan development may have been influenced by paraglacial processes (Sharp et al., 1959; Owen et al., 2003). This area, therefore, provides an opportunity to examine the interaction of climate, glaciation, hydrology, tectonics and autocyclic processes on alluvial fan development. We also compare our new alluvial fan record with other quantitative dating studies on alluvial fans in the American Southwest to test whether regional correlations can be made as a framework for future studies.

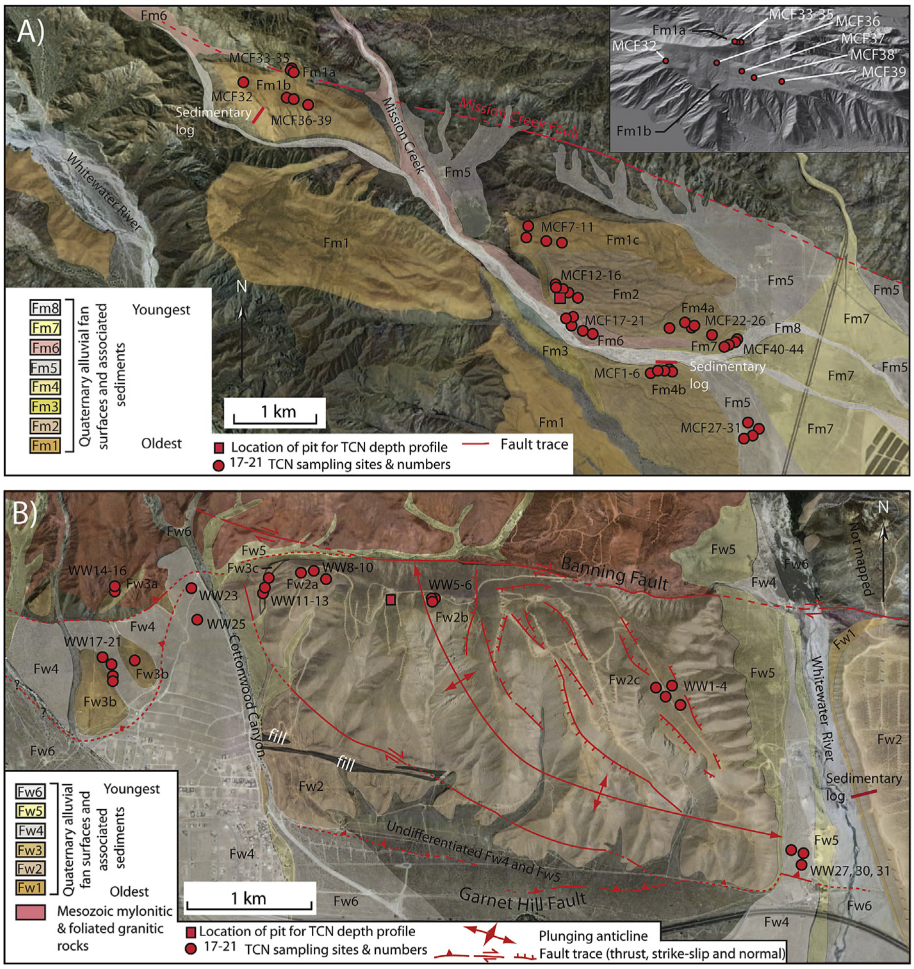

Fig. 2. Surficial geologic maps plotted on Google Earth images for A) the Mission Creek alluvial fan complex and B) Whitewater River alluvial fan complex showing the location of the sampling sites of terrestrial cosmogenic nuclide surface exposure dating. See Fig. 1C for the location of each detailed study area. The inset in the top right hand corner for part A is a LIDAR image for surface Fm1a and Fm1b (data from B4 project: http://www.siovizcenter.ucsd.edu/topo/b4.php). The trace of the Mission Creek fault in part A is modified from Allen (1957). The faults shown in part B are taken from Yule and Sieh (2003). The bold red lines next to surfaces Fm1 and Fm4 in part A) show the location of the graphic sedimentary logs in Fig. 4. In part B) the bold red line next to surface Fw2 shows the location of the graphic sedimentary log in Fig. 6. (For interpretation of the references to color in this figure legend, the reader is referred to the web version of this article.)

The alluvial fans in the American Southwest are amongst the best studied and are commonly used as analogues for alluvial fan studies in other regions. Yet, the ages and complex controls on their formation are not fully understood. Our studies provide one of the largest datasets of TCN ages on alluvial fans for any region of the American Southwest and it aims to elucidate the timing and nature of alluvial fan formation in the San Bernardino region of southern California. Furthermore, we aim to provide a framework for future geomorphic, tectonic, paleoenvironmental and archaeological studies on alluvial fans in the American Southwest and provide more robust analogues for studies in other regions.

2. Study area

The eastern end of the San Bernardino Mountains rise from the Salton Sea at 69 m below sea level in the Salton Trough to the top of San Gorgonio Mountain at 3506 m above sea level (asl) in <100 km (Fig. 1). The topography is essentially a consequence of transpressional uplift associated with a large bend in the San Andreas fault (Luyendyk, 1991; Blythe et al., 2000). The bedrock is a complex assemblage of juxtaposed far-traveled crystalline and sedimentary rocks ranging in age from Precambrian through Mesozoic (Matti et al., 1992a, b). The Mission Creek and Banning faults traverse the northern and southern margins of the eastern San Bernardino Mountains, respectively (Morton and Miller, 2003; Orozco, 2004; Orozco and Yule, 2003; Yule and Spotila, 2010; Yule et al., 2001; Yule, 2009: Figs. 1 and 2). The Mission Creek is a right lateral strike-slip fault and the Banning is an oblique strike-slip thrust fault, which converge at the eastern end of the Indio Hills to form a single strand of the San Andreas fault. Geomorphic (over 10^2–10^5 years) rates of displacement along the southernmost stretch of the San Andreas fault zone are in the order of 14–17 mm/a at Biskra Palms (van der Woerd et al., 2006; Behr et al., 2010; Fletcher et al., 2010).

Impressive alluvial fan complexes, covering an area of >50 km^2, are present around the mouths of the two major drainages, Mission Creek and Whitewater River (Fig. 1). These complexes comprise a succession of alluvial fans in which younger fans are inset into older ones (nested or telescopic in the sense of Bowman, 1978). Some of the alluvial fans form extensive surfaces that traverse and/or are displaced by faults in places and provide suitable landforms to apply TCN dating (Fig. 2).

The region is predominately influenced by a Pacific maritime climate. Oceanographic variability in both Pacific air pressure (El Nino Southern Oscillation) and sea surface temperature (Pacific Decadal Oscillations) has imposed considerable climate variability on the region during the 20th century and likely throughout the Quaternary (Hereford and Webb, 2002). Currently, the study area experiences a semi-arid to arid climate, with a mean annual precipitation of <63 mm/a (Stokes et al., 1997), but increasing gradually with elevation to reach 1270 mm/a above 2600 m asl (Sharp et al., 1959). Precipitation predominately takes the form of winter rain with occasional autumn storms encroaching from the tropical Pacific (Hunning, 1978). At elevations above 2600 m asl the majority of precipitation falls as snow (Sharp et al., 1959; Minnich, 1984, 1986). Climate data averaged from daily records recorded at the North Salton Sea weather station (33°33′N/115°55′W) between January 1, 1999 and August 4, 2002 show that mean annual temperatures range from 18 to 29 °C in the Coachella valley with maximum and minimum temperatures reaching 43 °C and 2 °C, respectively. These extremes in climate are reflected in the sparse desert vegetation that dominates the valley. Drought tolerant species such as desert scrub, creosote bush (*Larrea tridentata*), brittle bush (*Eucelia farinose*), Mormon tea (*Ephedra trifurca*), saltbush (*Atiplex* spp.) and tamarisk (*Tanarix* spp.) dominate the large expanses of alluvium whilst localized populations of cottonwood and willow cling to scattered springs and streams (McFadden, 1982; Salton Sea Authority, 2002). The soils in the region are semi-arid and thermic (McFadden, 1982). Paleoenvironmental conditions throughout the late Quaternary in the Mojave and Great Basin are discussed in much detail in Enzel et al. (2003), characterized by rapid changes from semi-arid to wetter climates on sub-Milankovitch timescales. Broadly, glacial times were characterized by wetter conditions, for example, Van Devender (1990) estimated that the Sonoran Desert (~300 km to the south East) was ~8 °C cooler and had ~100% more precipitation during the Last Glacial than today.

3. Methods

3.1. Field mapping

Alluvial fans were mapped in each study area in the field, aided by Google Earth images. Relative ages are assigned to each surface of the alluvial fans based on morphostratigraphy (Rawson et al., 2002) and relative weathering/erosion of surfaces and boulders. The mapped surfaces were numbered independently for each of the two drainages within their alluvial fan complexes (Fig. 2). For the Mission Creek alluvial fan complex individual surfaces were numbered Fm1 (oldest) through Fm8 (youngest), where the lower case "m" refers to the Mission Creek. Alluvial fan surfaces for the Whitewater River drainage system were numbers Fw1 (oldest) through Fw6 (youngest), where lower case "w" refers to the Whitewater River drainage. A lower case "a" (oldest), "b" or "c" were added to the alluvial fan surface name when major surfaces were subdivided (e.g. Fm1a, Fm1b and Fm1c). The faults and associated structures presented in Yule and Sieh (2003) for our Whitewater River study area were examined in the field; and we concur with their mapping and interpretation of the landforms and faults.

3.2. Terrestrial cosmogenic nuclide surface exposure dating

Samples for TCN dating were collected from quartz rich boulders (monagranites and gneiss) on individual alluvial fan surfaces by hammering off 400–500 g of the upper horizontal surface of each boulder (Fig. 3). The sampled boulders were located on elevated sites on the alluvial fan surfaces, and were deeply embedded, yet stood proud of the surface. Such boulders are most likely to have been deposited during the final stages of alluvial fan deposition and are likely to have retained their original position since deposition, without significant—if any—shielding by sediment cover. Where possible, we avoided sampling from any boulder that showed signs of weathering, such as exfoliation, granular disintegration, or splitting. Photographs were taken of each boulder and the degree of weathering and the site conditions were recorded (Tables 1 and 2). The inclination from the boulder site to the tops of the surrounding mountain ridges and peaks was measured to determine the potential effect of topographic shielding. By dating multiple boulders from each surface we aimed to qualitatively assess the likelihood of spurious ages due to weathering or inheritance of TCNs within boulders that may have experienced prior exposure. Meter-deep pits were dug into two surfaces in the study areas to collect samples for TCN depth profiles using the methods and rationale described by Anderson et al. (1996). The samples comprise ~1 kg of 1–5 cm size quartz-rich pebbles collected from 10 cm intervals in each of the pits. We undertook the depth profiles as a test for surface ages determined by the surface boulder dating.

Approximately 500 g of each sample was first crushed and sieved to separate out the 250–500 μm size fraction for further analysis. Clean quartz was isolated from each sample using HCl and HF:HNO_3 leaching (Kohl and Nishiizumi, 1992) and a Frantz magnetic separator. The pure quartz that was obtained was spiked with a beryllium carrier with a $^{10}Be/^{9}Be$ ratio of $2.99 \pm 0.22 \times 10^{-15}$ and dissolved in HF/HNO_3. After dissolution the sample was fumed to dryness three times with perchloric acid. The samples were run through anion and cation exchange resins to collect the Be fraction. Individual samples were then dried and ignited to produce BeO. The BeO was crushed with Nb powder and then loaded into aluminum cathodes for measurement with the accelerator mass spectrometer. The Accelerator Mass Spectrometry (AMS) measurements for the ^{10}Be were carried out at the Lawrence Livermore National Laboratory (LLNL) AMS facility.

All ^{10}Be exposure ages were calculated using the CRONUS calculator (version 2.2; Balco et al., 2008), which employs a ^{10}Be decay constant of $5.10 \pm 0.26 \times 10^{-7}$ per yr. The CRONUS calculator reports different exposure ages based on spallation scaling schemes as determined by Desilets and Zreda (2003, 2006), Dunai (2001), Lifton et al. (2001), and Lal (1991)/Stone (2000). We use ages calculated using the time-dependent model of Lal (1991) and Stone (2000), which uses a ^{10}Be production rate of 4.39 ± 0.37 atoms/g SiO_2/yr. This time-dependent model accounts for ^{10}Be production rate flux due to temporal changes in the geomagnetic field. For the two depth profiles, ^{10}Be concentrations and sample depths were analyzed. The method of Hidy et al. (2010), accessing ^{10}Be inheritance in sediment and erosion of the surface. This uses a comprehensive Monte Carlo simulations of TCN depth profiles for a particular study location which permits an explicit propagation of all error sources to calculated values for age, inheritance, and erosion rate. Probability distributions for pertinent parameters are chosen depending on what is already known, assumed to be known, or believed about the sampled site. Additionally, boundaries are placed on coupled parameters to remove unrealistic scenarios from the parameter solution spaces. Afterward, remaining unknowns are simulated within the framework designated by the selected options. We used the Matlab™ program of Hidy et al. (2010) that is easily modified to choose options and parameter distributions for each depth profile.

4. Geomorphology and sedimentology of study areas

4.1. Mission Creek alluvial fan complex

The Mission Creek alluvial fan complex is a set of nested/telescopic alluvial fans trending SE across the Mission Creek Fault and ESE into the Coachella Valley where it forms an active distal fan. The alluvial fan complex comprises six morphostratigraphically distinct ESE gently (2–4°) sloping surfaces, with each older surface being

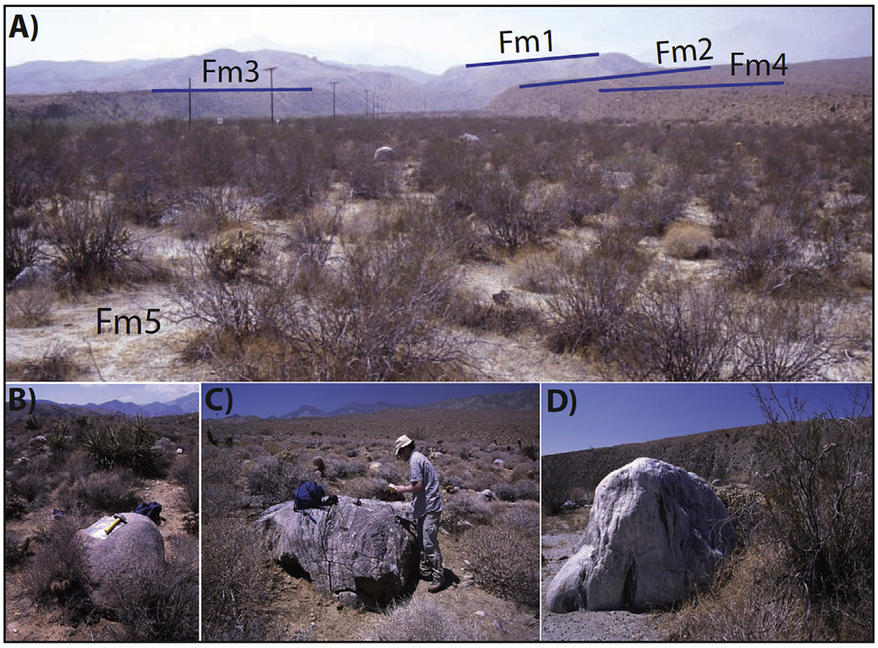

Fig. 3. View of selected alluvial fan surfaces and boulders on the Mission Creek alluvial fan complex. A) View looking west showing alluvial fan surfaces Fm1 through Fm5. Alluvial fan surfaces looking B) west across Fm1c showing sampled boulder MCF10, C) northwest across Fm4a showing sampled boulder MCF25, and D) north across Fm6 showing sampled boulder MCF18.

higher than the younger one below it, above the contemporary Mission Creek channel (Figs. 2 and 3A). The oldest alluvial fan (defined by surface Fm1), based on morphostratigraphy, is beheaded at its western end, to the immediate east of the Whitewater River drainage. Fm1 surface is undulating and denuded, rising >200 m above the contemporary Mission Creek drainage. The boulders on alluvial fan Fm1 surfaces are not very abundant and exhibited cavernous weathering and many are exfoliated. Boulders that appeared to be least weathered and stood highest were preferentially sampled on this surface (Fig. 3B). These included samples MCF33 to MCF35 and MCF32, MCF36 to MCF39 that were collected from two separate surfaces (Fm1a and Fm1b) from the upper part of alluvial fan Fm1 surface that had once been contiguous, and samples MCF7 to MCF11 that were collected from its surface lower in the study area (Fm1c; Fig. 2A). McFadden (1982) noted that soils on our alluvial fan Fm1 surface have a strongly developed red argillic horizon with substantial clay that forms continuous moderately-thick to thick clay films on grains and iron oxyhydroxides. All but the most resistant (fine grained quartz-rich lithologies) clasts were weathered and the soil lacks significant accumulations of carbonate. McFadden (1982) argued that these soil features are characteristic of soils that are 70,000–200,000 years old based on soil development.

Alluvial fan surface Fm2 is inset into alluvial fan surface Fm1 by ~100 m, and surface boulders are more abundant on Fm2 than on Fm1. Very subtle swale and bar forms (<1 m relief) are evident on alluvial fan surface Fm2. The Fm2 surface sits about 40 m above the present stream level. Boulder samples MCF12 to MCF16 were collected from the Fm2 surface and TCN depth profile samples (MCFA-1 to MCFA-6) were collected from a pit within the same surface.

Alluvial fan surface Fm3 is morphostratigraphically younger than alluvial fan surface Fm2. It is inset into Fm2, and sits about 25–30 m above the present stream level. However, no samples were collected from this surface because of limited resources to process them.

The alluvial fan surfaces of Fm4 rise about 15–25 m above the present stream level. Two sets of samples (MCF1 to MCF6 and MCF22 to MCF26) were collected from Fm4 on opposite sides of the Mission Creek drainage (Fm4a to the north and Fm4b to the south of Mission Creek). These boulders showed little signs of weathering and it was difficult to sample them because they were very strongly indurated (Fig. 3C). McFadden (1982) classified the soils on alluvial fans Fm2, Fm3 and Fm4 as Xeralfic Haplargids. As McFadden (1982) noted, the soil has moderately to strongly developed argillic horizons that lack structural development because of their gravelly nature, a yellowish to reddish brown B horizon, significant amounts of iron oxyhydroxides in the A and B horizons, and carbonate accumulation in both the basal B and Cca horizons (coating large particles, and as filaments and veins in the soil matrix). McFadden (1982) argued that the soils were about 13,000–70,000 years old based on their soil development.

Alluvial fan surface Fm5 sits <10 m above the present stream level and is inset into the alluvial fan surfaces of Fm4. The Fm5 alluvial fan surface has abundant boulders that stand high and exhibit little, if any, weathering. Distinct bar and swale features (~1 m high) are evident on this surface. Samples MCF27–31 were collected from this surface and these were extremely hard to sample because of the lack of weathering.

The Fm6 alluvial fan surface can be traced up the Mission Creek drainage throughout the mapped area and sits a few meters above the present stream to form a distinct terrace. Samples MCF17–21 were collected from this surface (Fig. 3D).

The youngest alluvial fan surface, Fm7, is inset into alluvial fan surfaces Fm6 and Fm5. The Fm7 alluvial fan surface has abundant large fresh boulders and distinct bar and swales forms. Samples MCF40–44 were collected from this surface. Soils on the Fm5, Fm6, and Fm7 alluvial fan surfaces are poorly developed and organic matter-rich A and Cox horizons are not present, but there is an incipient calcic horizon forming at a depth of 35–185 cm; McFadden (1982) classifies the soils as Xeric Torriorthent since they form in a moist region that approaches xeric and argues they are

Table 1
Sample descriptions, locations, and ^{10}Be terrestrial cosmogenic nuclide concentration and ages.

Sample number	Rock type	Boulder size long axis/intermediate axis/height (cm)	Degree of weathering[a]	Latitude °N	Longitude °W	Altitude (m asl)	Quartz mass (g)	Be carrier (mg/g)	Be (g)	^{10}Be/^{9}Be $\times 10^{-15}$	^{10}Be concentration (10^6 atoms/g)	^{10}Be age (ka) Desilets et al. (2003/2006)	^{10}Be age (ka) Dunai (2001)	^{10}Be age (ka) Lifton et al. (2005)	^{10}Be age (ka) Lal (1991)/Stone (2000) Time-independent	^{10}Be age (ka) Lal (1991)/Stone (2000) Time-dependent
Mission Creek Alluvial Fan Complex																
Fm7																
MCF40	Gniess	400/230/200	N	33.9973	116.5923	583	41.7800	0.889	0.5192	16.8 ± 3.2	0.0124 ± 0.002	2.19 ± 0.44	2.11 ± 0.42	2.17 ± 0.41	1.80 ± 0.33	1.91 ± 0.35
MCF41	Gniess	400/250/175	N	33.9974	116.5925	577	38.4600	0.889	0.5186	28.0 ± 3.4	0.0224 ± 0.003	4.02 ± 0.72	3.91 ± 0.70	3.98 ± 0.66	3.27 ± 0.52	3.49 ± 0.55
MCF42	Gniess	240/170/70	N	33.9976	116.5924	576	40.0500	0.889	0.5211	5.4 ± 3.1	0.0042 ± 0.002	0.68 ± 0.34	0.67 ± 0.33	0.68 ± 0.33	0.61 ± 0.30	0.61 ± 0.29
MCF44	Porphyritic Granite	120/120/40	N	33.9973	116.5916	574	31.4400	0.889	0.5039	5.9 ± 3.1	0.0056 ± 0.003	0.94 ± 0.51	0.91 ± 0.50	0.93 ± 0.50	0.82 ± 0.44	0.83 ± 0.45
														Mean age	**1.62 ± 1.21**	**1.71 ± 1.32**
Fm6																
MCF17	Granite	180/120/80	L	34.0009	116.6117	653	34.5600	0.889	0.5184	44.1 ± 3.5	0.0394 ± 0.003	6.15 ± 0.68	6.04 ± 0.85	6.08 ± 0.76	5.43 ± 0.63	5.52 ± 0.63
MCF18	Gniess	400/300/180	L	34.0009	116.6112	653	24.9200	0.389	0.9984	12.2 ± 2.4	0.0127 ± 0.002	2.12 ± 0.42	2.04 ± 0.40	2.10 ± 0.39	1.75 ± 0.32	1.86 ± 0.33
MCF18D			L	34.0009	116.6112	653	46.9800	0.889	0.5158	14.8 ± 3.2	0.0096 ± 0.002	1.58 ± 0.38	1.52 ± 0.36	1.57 ± 0.36	1.32 ± 0.30	1.39 ± 0.31
MCF19	Granite	170/170/50	L	33.9995	116.6093	645	21.0358	0.889	0.5142	10.0 ± 10.0	0.0145 ± 0.015	2.45 ± 2.56	2.36 ± 2.46	2.43 ± 2.53	2.01 ± 2.09	2.14 ± 2.22
MCF20	Granite	200/180/60	L	33.9998	116.6104	651	22.5744	0.889	0.5100	10.0 ± 10.0	0.0135 ± 0.013	2.27 ± 2.20	2.18 ± 2.12	2.24 ± 2.17	1.86 ± 1.80	1.98 ± 1.92
MCF21	Gniess	230/180/130	E	34.0004	116.6113	658	43.2100	0.889	0.5181	69.1 ± 3.9	0.0493 ± 0.003	7.45 ± 0.99	7.34 ± 0.97	7.35 ± 0.85	6.77 ± 0.72	6.70 ± 0.70
														Mean age	**3.19 ± 2.30**	**3.27 ± 2.25**
Fm5																
MCF27	Granite	100/90/50	L	33.9884	116.5868	532	29.1789	0.389	1.0534	48.4 ± 8.2	0.0455 ± 0.008	7.63 ± 1.62	7.49 ± 1.59	7.51 ± 1.52	6.87 ± 1.35	6.80 ± 1.33
MCF27D			L	33.9884	116.5868	532	55.7100	0.889	0.5260	29.2 ± 3.4	0.0164 ± 0.002	3.10 ± 0.53	2.99 ± 0.51	3.06 ± 0.48	2.47 ± 0.37	2.64 ± 0.39
MCF28	Metagranite	150/120/80	L	33.9884	116.5868	534	45.3900	0.889	0.5178	37.2 ± 3.9	0.0252 ± 0.003	4.61 ± 0.77	4.49 ± 0.75	4.56 ± 0.71	3.80 ± 0.56	4.00 ± 0.58
MCF29	Leucogranite	90/70/45	L	33.9880	116.5875	531	26.2437	0.389	1.0214	23.0 ± 10.1	0.0233 ± 0.010	4.30 ± 1.92	4.19 ± 1.87	4.26 ± 1.88	3.52 ± 1.54	3.73 ± 1.64
MCF30	Metagranite	150/100/40	L	33.9879	116.5882	541	36.3200	0.889	0.5235	39.3 ± 3.5	0.0337 ± 0.003	5.84 ± 0.86	5.72 ± 0.84	5.78 ± 0.77	5.05 ± 0.63	5.18 ± 0.64
MCF31	Granite	100/90/35	L	33.9891	116.5879	541	48.1400	0.889	0.5018	77.8 ± 3.9	0.0482 ± 0.002	8.03 ± 1.01	7.88 ± 0.98	7.91 ± 0.85	7.23 ± 0.70	7.14 ± 0.67
														Mean age	**4.82 ± 1.91**	**4.92 ± 1.79**
Fm4b																
MCF1	Granite	110/100/90	L, C	33.9983	116.5831	610	15.6002	0.440	1.0632	249.7 ± 6.4	0.5011 ± 0.0129	74.39 ± 9.15	72.05 ± 8.82	71.98 ± 7.47	72.49 ± 6.67	67.55 ± 6.06
MCF2	Granite	200/60/50	L, C	33.9953	116.5985	610	15.2688	0.440	1.0822	212.6 ± 7.1	0.4435 ± 0.0148	65.92 ± 8.22	64.00 ± 7.94	63.92 ± 6.77	64.11 ± 6.07	60.00 ± 5.53
MCF3	Granite	110/100/100	M, E, C	33.9955	116.5992	610	15.3620	0.440	1.1081	219.2 ± 7.6	0.4654 ± 0.0161	68.95 ± 8.62	66.90 ± 8.32	66.81 ± 7.09	67.21 ± 6.37	62.80 ± 5.80
MCF4	Granite	210/100/60	M, E	33.9950	116.6000	619	15.0557	0.440	1.1065	215.2 ± 5.7	0.4656 ± 0.0122	68.59 ± 8.42	66.56 ± 8.13	66.47 ± 6.89	66.88 ± 6.16	62.49 ± 5.59
MCF5	Granite	200/100/100	M, C	33.9953	116.5989	618	15.3212	0.440	1.1122	222.4 ± 7.9	0.4753 ± 0.0170	69.97 ± 8.77	67.86 ± 8.47	67.77 ± 7.23	68.25 ± 6.52	63.73 ± 5.92
MCF6	Gneiss	230/200/50	M, E, C	33.9954	116.5981	614	15.4245	0.440	1.0910	219.2 ± 8.3	0.4566 ± 0.0172	67.57 ± 8.50	65.58 ± 8.21	65.50 ± 7.01	65.82 ± 6.32	61.53 ± 5.76
														Mean age	**67.46 ± 2.84**	**63.01 ± 2.57**
Fm4a																
MCF22	Granite	230/120/80	M-H, E	33.9987	116.5935	590	21.9932	0.389	1.0281	271.7 ± 13.2	0.3320 ± 0.0088	49.20 ± 6.03	47.76 ± 5.82	47.56 ± 4.92	48.48 ± 4.47	44.80 ± 4.01
MCF23	Granite	200/190/80	L, C	33.9999	116.5958	600	22.2400	0.389	1.0615	385.1 ± 13.2	0.4784 ± 0.016	71.56 ± 8.93	69.34 ± 8.61	69.26 ± 7.34	69.69 ± 6.60	65.07 ± 6.00
MCF24	Granite	250/200/70	M, E	33.9998	116.5960	601	23.3400	0.389	1.0761	360.7 ± 9.2	0.4329 ± 0.011	64.79 ± 7.94	62.89 ± 7.67	62.82 ± 6.50	62.91 ± 5.78	58.84 ± 5.26
MCF25	Gniess	320/220/100	L, C	33.9997	116.5981	607	21.7540	0.389	1.0278	409.9 ± 10.2	0.5041 ± 0.013	75.03 ± 9.23	72.69 ± 8.90	72.63 ± 7.54	73.11 ± 6.75	68.12 ± 6.11
MCF26	Quartzite	250/180/90	L	34.0003	116.5966	601	14.5477	0.389	1.0225	251.1 ± 12.1	0.4594 ± 0.022	68.63 ± 8.89	66.59 ± 8.58	66.52 ± 7.41	66.83 ± 6.74	62.49 ± 6.15
														Mean age	**64.20 ± 9.56**	**59.86 ± 9.09**
Fm2																
MCF12	Granite	160/100/50	M, E	34.0048	116.6128	740	16.8200	0.389	1.0078	287.7 ± 10.0	0.4487 ± 0.016	59.97 ± 7.50	58.12 ± 7.23	57.90 ± 6.16	58.69 ± 5.59	54.32 ± 5.04
MCF13	Granite	180/100/50	L	34.0048	116.6126	736	14.1500	0.389	1.0310	369.9 ± 9.3	0.7015 ± 0.018	94.27 ± 11.65	91.35 ± 11.23	91.28 ± 9.51	92.82 ± 8.61	86.06 ± 7.75
MCF14	Granite	100/80/70	M, E	34.0046	116.6122	740	23.8500	0.389	1.0513	533.6 ± 13.4	0.6122 ± 0.015	81.91 ± 10.07	79.25 ± 9.69	79.10 ± 8.20	80.52 ± 7.42	74.59 ± 6.67
MCF15	Granite	120/60/50	L	34.0045	116.6116	730	22.1300	0.389	1.0280	390.3 ± 10.0	0.4720 ± 0.0121	63.57 ± 7.79	61.71 ± 7.53	61.54 ± 6.36	62.26 ± 5.72	57.92 ± 5.17
MCF16	Granite	140/120/80	M	34.0041	116.6109	718	18.9988	0.389	1.0224	342.1 ± 12.3	0.4792 ± 0.0173	65.11 ± 8.15	63.23 ± 7.88	63.07 ± 6.71	63.80 ± 6.08	59.43 ± 5.52
														Mean age	**71.62 ± 14.53**	**66.46 ± 13.42**
Fm1c																
MCF7	Granite	160/100/40	M, E	34.0108	116.6176	813	23.5565	0.389	1.0278	319.2 ± 8.2	0.3625 ± 0.009	44.65 ± 5.44	43.52 ± 5.28	43.26 ± 4.45	44.76 ± 4.09	41.25 ± 3.66
MCF8	Granite	190/120/100	M	34.0100	116.6182	806	24.3902	0.389	1.0281	453.2 ± 11.2	0.4972 ± 0.012	62.95 ± 7.70	61.12 ± 7.44	60.89 ± 6.27	61.98 ± 5.68	57.48 ± 5.11
MCF9	Granite	100/100/60	M, E	34.0099	116.6181	804	25.1231	0.389	1.0209	421.2 ± 17.3	0.4455 ± 0.018	56.24 ± 7.11	54.40 ± 6.85	54.10 ± 5.84	55.52 ± 5.39	51.00 ± 4.83
MCF10	Granite	130/80/50	M-H	34.0098	116.6161	797	25.6600	0.389	1.0357	446.0 ± 11.3	0.4685 ± 0.012	59.76 ± 7.32	57.92 ± 7.06	57.65 ± 5.96	58.74 ± 5.40	54.24 ± 4.84
MCF11	Granite	300/150/250	L, C	34.0089	116.6143	773	19.8400	0.389	1.0940	267.7 ± 7.1	0.3842 ± 0.010	48.93 ± 5.98	47.53 ± 5.78	47.23 ± 4.87	48.92 ± 4.49	44.86 ± 4.00
														Mean age	**53.98 ± 7.06**	**49.76 ± 6.66**

(*continued on next page*)

Table 1 (*continued*)

Sample number	Rock type	Boulder size long axis/intermediate axis/height (cm)	Degree of weathering[a]	Latitude °N	Longitude °W	Altitude (m asl)	Quartz mass (g)	Be carrier (mg/g)	Be (g)	^{10}Be/^{9}Be $\times 10^{-15}$	^{10}Be concentration (10^{6} atoms/g)	^{10}Be age (ka) Desilets et al. (2003/2006)	^{10}Be age (ka) Dunai (2001)	^{10}Be age (ka) Lifton et al. (2005)	^{10}Be age (ka) Lal (1991)/Stone (2000) Time-independent	^{10}Be age (ka) Lal (1991)/Stone (2000) Time-dependent
Fm1b																
MCF32	Granite	200/120/50	M, E	34.0262	116.6544	1067	26.1000	0.389	1.0524	111.1 ± 4.8	0.1166 ± 0.005	12.87 ± 1.62	12.61 ± 1.58	12.61 ± 1.58	11.86 ± 1.15	11.70 ± 1.11
MCF36	Granite	320/230/90	M	34.0258	116.6507	1035	22.0500	0.389	1.0152	181.0 ± 11.1	0.2169 ± 0.013	23.84 ± 3.17	23.22 ± 3.08	23.22 ± 3.08	22.63 ± 2.40	21.90 ± 2.28
MCF37	Granite	230/150/70	M	34.0249	116.6491	1017	22.2700	0.389	1.0134	278.5 ± 12.2	0.3298 ± 0.014	35.54 ± 4.49	34.58 ± 4.35	34.58 ± 4.35	34.97 ± 3.41	32.89 ± 3.13
MCF38	Granite	180/100/60	M	34.0246	116.6486	1011	22.9100	0.389	1.0202	220.3 ± 6.1	0.2553 ± 0.007	28.24 ± 3.44	27.48 ± 3.34	27.48 ± 3.34	27.14 ± 2.49	26.00 ± 2.32
MCF39	Granite	260/170/160	M, E	34.0243	116.6467	997	24.2800	0.389	1.0122	352.4 ± 13.4	0.3824 ± 0.015	40.93 ± 5.14	39.95 ± 4.99	39.95 ± 4.99	41.21 ± 3.97	38.18 ± 3.60
														Mean age	**27.56 ± 11.32**	**26.12 ± 10.20**
Fm1a																
MCF33	Granite	170/150/50	M, E	34.0280	116.6498	1092	21.5900	0.389	1.0093	605.2 ± 17.7	0.7364 ± 0.022	73.91 ± 9.16	71.69 ± 8.84	71.69 ± 8.84	74.69 ± 6.97	68.42 ± 6.22
MCF34	Granite	200/180/40	M	34.0280	116.6497	1085	19.5242	0.389	1.0232	248.8 ± 11.9	0.3394 ± 0.016	34.75 ± 4.45	33.80 ± 4.31	33.80 ± 4.31	34.28 ± 3.41	32.21 ± 3.14
MCF35	Granite	220/200/60	M, E, C	34.0280	116.6495	1086	23.9000	0.389	1.0199	451.5 ± 14.9	0.5015 ± 0.017	49.65 ± 6.17	48.22 ± 5.96	48.22 ± 5.96	50.78 ± 4.80	46.00 ± 4.23
														Mean age	**53.24 ± 20.33**	**48.87 ± 18.28**
White Water Alluvial Fan Complex																
Fw4b																
WW27	Quartzite	110/90/60	M	33.9269	116.6404	442	24.1394	0.389	1.0355	38.1 ± 10.5	0.0425 ± 0.0117	7.69 ± 2.31	7.54 ± 2.26	7.58 ± 2.22	6.89 ± 2.00	6.83 ± 1.97
WW30	Quartzite	110/70/35	N	33.9279	116.6401	450	24.7781	0.389	1.0026	30.1 ± 10.4	0.0317 ± 0.0109	5.91 ± 2.15	5.79 ± 2.11	5.85 ± 2.10	5.10 ± 1.81	5.23 ± 1.86
WW31	Gneiss	100/50/40	N	33.9281	116.6411	447	23.4900	0.389	1.0494	25.1 ± 10.2	0.0291 ± 0.0118	5.54 ± 2.34	5.41 ± 2.29	5.49 ± 2.29	4.70 ± 1.95	4.86 ± 2.01
														Mean age	**5.56 ± 1.16**	**5.64 ± 1.05**
Fw4a																
WW23	Gneiss	320/180/80	M	33.9471	116.6934	585	33.2102	0.389	1.0679	30.3 ± 10.5	0.0254 ± 0.0088	4.47 ± 1.64	4.36 ± 1.60	4.43 ± 1.60	3.68 ± 1.32	3.90 ± 1.39
WW25	Metaquartzite	130/40/30	N	33.9449	116.6929	565	25.4319	0.389	1.0088	389.7 ± 13.9	0.4024 ± 0.0144	62.19 ± 7.78	60.30 ± 7.51	60.25 ± 6.41	60.10 ± 5.73	56.15 ± 5.21
																n/a
Fw3c																
WW11	Granite	200/150/50	M, E	33.9479	116.6866	601	15.4273	0.389	1.0291	14.5 ± 10.1	0.0251 ± 0.0175	4.38 ± 3.11[b]	4.27 ± 3.03[b]	4.34 ± 3.06[b]	3.60 ± 2.54[b]	3.82 ± 2.69[b]
WW12	Granite	150/120/45	H	33.9472	116.6870	591	25.2480	0.389	1.1243	251.9 ± 8.4	0.2920 ± 0.0097	43.31 ± 5.36	42.21 ± 5.20	42.07 ± 4.42	42.58 ± 4.00	39.73 ± 3.64
WW13	Granite	95/85/40	M	33.9468	116.6871	583	20.1569	0.389	1.0611	234.9 ± 6.4	0.3218 ± 0.0087	47.94 ± 5.87	46.58 ± 5.68	46.39 ± 4.80	47.27 ± 4.35	43.74 ± 3.92
														Mean age	**44.92 ± 3.32**	**41.74 ± 2.83**
Fw3b																
WW17	Quartzite	180/110/25	L	33.9405	116.7000	525	18.3456	0.389	1.0296	347.9 ± 8.7	0.5082 ± 0.0128	81.27 ± 10.00	78.58 ± 9.62	78.64 ± 8.16	78.62 ± 7.25	73.45 ± 6.58
WW18	Quartzite	80/40/25	L, C	33.9408	116.7000	529	26.4651	0.389	1.0314	406.0 ± 12.8	0.4118 ± 0.0130	65.48 ± 8.13	63.54 ± 7.85	63.53 ± 6.68	63.28 ± 5.94	59.35 ± 5.42
WW19	Quartzite	85/55/15	M	33.9417	116.7000	541	26.6192	0.389	1.0470	419.6 ± 14.7	0.4296 ± 0.0151	67.55 ± 8.45	65.54 ± 8.16	65.51 ± 6.97	65.44 ± 6.23	61.34 ± 5.69
WW20	Gneiss	70/45/20	L	33.9417	116.7000	536	20.9307	0.389	1.0206	335.2 ± 8.4	0.4254 ± 0.0107	67.17 ± 8.24	65.18 ± 7.95	65.16 ± 6.74	65.04 ± 5.98	61.00 ± 5.45
WW21	Gneiss	120/45/20	L	33.9418	116.6983	540	19.2018	0.389	1.0112	243.6 ± 11.9	0.3340 ± 0.0164	51.95 ± 6.72	50.27 ± 6.48	50.12 ± 5.59	50.72 ± 5.12	46.92 ± 4.63
														Mean age	**64.62 ± 9.90**	**60.41 ± 9.41**
Fw3a																
WW14	Granite	150/90/30	H	33.9472	116.7000	654	21.5898	0.389	1.0167	170.8 ± 5.8	0.2093 ± 0.0071	30.71 ± 3.80[b]	29.78 ± 3.67[b]	29.91 ± 3.14[b]	29.01 ± 2.73[b]	27.86 ± 2.55[b]
WW15	Granite	100/40/25	H	33.9472	116.7000	645	24.0391	0.389	1.0207	371.0 ± 17.0	0.4100 ± 0.0188	59.27 ± 7.61	57.39 ± 7.34	57.24 ± 6.31	57.61 ± 5.74	53.43 ± 5.19
WW16	Gneiss	50/25/25	H	33.9469	116.7000	659	19.3032	0.389	1.0624	269.5 ± 12.0	0.3861 ± 0.0172	54.76 ± 7.00	52.96 ± 6.74	52.76 ± 5.79	53.64 ± 5.31	49.41 ± 4.77
														Mean age	**55.62 ± 2.81**	**51.42 ± 2.84**
Fw2c																
WW01	Granite	200/120/100	L	33.9386	116.6508	712	26.1056	0.389	1.0536	409.9 ± 16.5	0.4306 ± 0.0173	58.90 ± 7.45	57.03 ± 7.18	56.82 ± 6.14	57.56 ± 5.59	53.21 ± 5.04
WW02	Granite	200/100/70	L	33.94	116.6515	731	27.0495	0.389	1.0371	567.1 ± 11.2	0.5659 ± 0.0112	76.16 ± 9.28	73.78 ± 8.95	73.62 ± 7.54	74.91 ± 6.80	69.40 ± 6.11
WW03	Granite	230/140/60	L	33.9392	116.6521	736	26.0856	0.389	1.0369	299.4 ± 12.7	0.3098 ± 0.0131	41.02 ± 5.19	39.99 ± 5.04	39.88 ± 4.32	40.51 ± 3.96	37.82 ± 3.60
WW04	Granite	250/190/90	M, E	33.9399	116.6529	747	26.5442	0.389	1.0211	475.2 ± 12.0	0.4758 ± 0.0120	63.27 ± 7.75	61.42 ± 7.49	61.23 ± 6.33	62.04 ± 5.70	57.64 ± 5.15
														Mean age	**58.75 ± 14.22**	**54.51 ± 13.06**
Fw2b																
WW05	Granite	120/70/35	M, E	33.9462	116.6724	809	24.8256	0.389	1.0076	401.7 ± 14.2	0.4244 ± 0.0150	53.02 ± 6.61	51.31 ± 6.37	50.99 ± 5.41	52.72 ± 5.01	48.22 ± 4.46
WW06	Granite	120/90/20	M, E	33.9464	116.6724	804	26.2166	0.389	1.0115	415.7 ± 11.7	0.4175 ± 0.0117	52.27 ± 6.42	50.60 ± 6.19	50.28 ± 5.22	52.04 ± 4.81	47.71 ± 4.31
WW07	Granite	120/70/20	H, E	33.9463	116.6724	805	25.9424	0.389	1.0301	725.6 ± 17.3	0.7499 ± 0.0179	95.28 ± 11.74	92.38 ± 11.33	92.24 ± 9.57	94.40 ± 8.71	87.29 ± 7.82
														Mean age	**66.39 ± 24.26**	**61.04 ± 22.74**
Fw2a																
WW08	Granite	180/110/60	H	33.9478	116.6816	686	23.6926	0.389	1.0320	472.3 ± 15.5	0.5355 ± 0.0176	74.74 ± 9.32	72.40 ± 8.99	72.27 ± 7.65	73.26 ± 6.93	68.03 ± 6.26
WW09	Pegmatite	220/170/70	L	33.9484	116.6827	671	22.9572	0.389	1.1163	333.5 ± 13.2	0.4221 ± 0.0168	59.75 ± 7.55	57.87 ± 7.28	57.71 ± 6.22	58.18 ± 5.64	53.93 ± 5.09
WW10	Granite	160/100/40	M	33.9483	116.6838	661	49.9918	0.389	1.0702	693.6 ± 20.1	0.3865 ± 0.0112	54.72 ± 6.74	52.93 ± 6.48	52.72 ± 5.49	53.61 ± 4.98	49.38 ± 4.46
														Mean age	**61.68 ± 10.28**	**57.11 ± 9.72**

		Depth (cm)										Bayesian most probably (ka)	Bayesian 2 sigma upper (ka)	Bayesian 2 sigma lower (ka)	Inheritance (10^4 atoms SiO_2/g)	Erosion rate (cm/ka)
Mission Creek Depth Profile – Surface Fm2																
MCFA-1	Sediment	30–40	n/a	34.0100	116.6182	806	24.5325	0.389	1.1126	124.5 ± 3.8	0.1471 ± 0.0044					
MCFA-2	Sediment	40–50	n/a	34.0100	116.6182	806	24.2133	0.389	1.0513	135.2 ± 4.1	0.1529 ± 0.0047					
MCFA-3	Sediment	50–60	n/a	34.0100	116.6182	806	22.6946	0.389	1.0362	104.2 ± 3.6	0.1240 ± 0.0042					
MCFA-4	Sediment	60–70	n/a	34.0100	116.6182	806	26.1025	0.389	1.0085	127.3 ± 4.0	0.1282 ± 0.0040					
MCFA-5	Sediment	70–80	n/a	34.0100	116.6182	806	24.5013	0.389	1.0312	73.8 ± 3.1	0.0809 ± 0.0034					
MCFA-6	Sediment	80–90	n/a	34.0100	116.6182	806	29.4047	0.389	1.0877	94.2 ± 3.7	0.0908 ± 0.0035	48.7	65.6	36.8	4.80	0.47
Whitewater Depth Profile – Surface Fw2b																
WWFA-1	Sediment	30–40	n/a	33.9484	116.6827	671	13.2295	0.389	1.0482	125.0 ± 3.7	0.2580 ± 0.0075					
WWFA-2	Sediment	40–50	n/a	33.9484	116.6827	671	16.7803	0.389	1.0307	134.9 ± 3.9	0.2159 ± 0.0063					
WWFA-3	Sediment	50–60	n/a	33.9484	116.6827	671	16.4110	0.389	1.2080	108.8 ± 3.4	0.2086 ± 0.0065					
WWFA-4	Sediment	60–70	n/a	33.9484	116.6827	671	18.1628	0.389	1.0226	126.4 ± 5.2	0.1854 ± 0.0076					
WWFA-5	Sediment	70–80	n/a	33.9484	116.6827	671	19.9122	0.389	1.0125	117.4 ± 4.3	0.1555 ± 0.0057					
WWFA-6	Sediment	80–85	n/a	33.9484	116.6827	671	19.9630	0.389	1.1304	109.7 ± 4.0	0.1619 0.0058	53.9	72.9	40.9	4.75	0.42

[a] Weathering (N – none; L – Low; M – moderate; H – High); C – Cracked; E – Exfoliated.
[b] Age not used in calculation of mean age.

younger than ~7000 years. The active alluvial fans/streams are grouped into Fm8 and are characterized by abundant sandy and pebbly stretches, with abundant meter-size boulders and no soil development, and very prominent bars and channels.

Where exposures are present within each of the alluvial fans it is apparent that the sedimentology of each is very similar. The sediments comprise decimeter- to meter-thick gradational beds of gravels and boulders that slope sub-parallel to the alluvial fan surfaces (Fig. 4A). Meter-wide and decimeter-deep pebbly sand channel fills are present within some of the sections; although these form a minor component of the alluvial fans. One of the best exposures through the alluvial fan sediments is present in alluvial fan surface Fm4b on the southern side of Mission Creek (33°59.784′N/116°35.834′W; Fig. 4B). A dark reddish (5YR 4/4) buried soil is present at this location exhibiting a moderately well developed argillaceous horizon with deeply weathered boulders. McFadden (1982) classified this buried soil as a Haploxeralfic Haplargid.

4.2. Whitewater River alluvial fan complex

The alluvial fans within the Whitewater River study form a nested/telescopic succession around the mouths of Whitewater River and Cottonwood Canyon (Figs. 2B and 5). The oldest alluvial fan surface (Fw1) is only exposed along the eastern edge of Whitewater River where it underlies deposits of Fw2 (Fig. 5B). The top of the sediments is marked by a distinct dark reddish (5YR 4/4) buried soil with a well-developed argillaceous horizon with deeply weathered boulders.

Alluvial fan surface Fw2 forms an extensive area that rises 80–100 m above the active channel of the Whitewater River and becomes several tens of meters lower towards the west. The alluvial fan is sandwiched between the Banning right-lateral strike-slip fault to the north and the dextral-oblique Garnet Hill Fault to the south (Fig. 2B). Allen (1957) refers to these alluvial fan deposits are the Cabezon fanglomerates, and Yule and Sieh (2003) refer to them as the Cabezon Formation and suggest that they are older than 100,000 years on the basis of what they describe as extreme development of a capping soil, although they do not describe the soils in any detail. The alluvial fan sediments are deformed by the strike-slip and oblique-slip/thrust faults and are folded by an active anticline expressed slightly by a broad east–west hilly terrane (Fig. 2B). A series of NNW trending scarps traverse the deposits at their eastern end. The surface has shattered boulders that exhibit slight cavernous weathering, and very subtle bar and swale features (<1 m high) are present. Samples (WW1 to WW10) for TCN were collected from three areas on the alluvial fan (Fw2a, Fw2b and Fw2c; Figs. 2B and 5A) to test whether there was any systematic difference in age between these surfaces that might be related to displacement along the Banning fault (Fig. 5A, C). In addition, a pit was dug into the Fw2b surface to obtain samples for a TCN depth profile (WWFA-1 to WWFA-6). The soils have moderately to strongly developed argillic horizons that lack structural development because of their gravelly nature and have a reddish brown B horizon. Many of the clasts are weathered and iron oxyhydroxides are abundant. Clasts within the Fm2 alluvial fans are sourced from the headwaters of the Whitewater River from rocks north of the Mission Creek Fault (Allen, 1957; Matti et al., 1985, 1992a; Matti and Morton, 1993).

The next youngest alluvial fan surface, Fw3, is inset into alluvial fan surface Fw2 at its western end. The Fw3 surface occurs as isolated patches to the far west of the Whitewater River study area. The surface is faulted at several locations. Rare boulders, many exhibiting granular weathering, are present on its surface, grus is abundant, and bar and swale features are very subtle (Fig. 5D).

Table 2
Summary of ^{10}Be ages using the Lal (1991)/Stone (2000) time-dependent scaling model for surfaces in each of the detailed study areas (MIS = marine oxygen isotope stage).

Alluvial fan complex	Alluvial fan surface		Number of samples	Average age[a] (ka)	Maximum age[b] (ka)	Range of ^{10}Be ages (ka)	Assigned likely age (ka)
Mission Creek	Fm7		4	1.7 ± 1.3	3.5 ± 0.6	0.6–3.5	Historical/Active
	Fm6		6	3.3 ± 2.3	6.7 ± 0.7	1.4–6.7	Holocene
	Fm5		6	4.9 ± 1.8	7.1 ± 0.7	2.6–7.1	Holocene
	Fm4	Fm4b	6	63.0 ± 2.6	67.6 ± 6.1	60.0–67.6	MIS 4
		Fm4a	5	59.9 ± 9.1	68.1 ± 6.1	44.8–68.1	MIS 4
	Fm3		Not dated				MIS 4
	Fm2		5	66.5 ± 13.4	86.1 ± 7.8	54.3–86.1	MIS 4
	Fm2		Depth profile	$48.7^{+16.9}/_{-11.9}$	65.6	36.8–65.6	MIS 4
	Fm1	Fm1c	5	49.7 ± 6.7	57.5 ± 5.1	41.2–57.5	>MIS 4
		Fm1b	5	26.1 ± 10.2	38.2 ± 3.6	11.7–38.2	>MIS 4
		Fm1a	3	48.9 ± 18.2	68.4 ± 6.2	32.2–68.4	>MIS 4
Whitewater	Fw6		Not dated				Historical/Active
	Fw5		Not dated				Late Holocene
	Fw4	Fw4b	3	5.6 ± 1.1	6.8 ± 2.0	4.9–6.8	Holocene
		Fw4a	2	n/a	56.2 ± 5.2	3.9–56.2	Holocene
	Fw3	Fw3c	3	41.7 ± 2.8	43.7 ± 3.9	39.7–43.7[c]	≥MIS 3
		Fw3b	5	60.4 ± 9.4	73.5 ± 6.6	46.9–73.5	MIS 4
		Fw3a	3	51.4 ± 2.8	53.2 ± 5.0	49.4–53.4[d]	MIS 4
	Fw2	Fw2c	4	54.5 ± 13.1	69.4 ± 6.1	37.8–69.4	≥MIS 4
		Fw2b	3	61.0 ± 22.7	87.3 ± 7.8	47.6–87.3	≥MIS 4
		Fw2a	3	57.1 ± 9.7	68.0 ± 6.3	54.0–68.0	≥MIS 4
		Fw2a	Depth profile	$53.9^{+19.0}/_{-13.0}$	72.9	40.9–53.9	MIS 4
	Fw1		Not dated				>MIS 4

[a] Uncertainty expressed as 1 σ.
[b] Based on oldest ^{10}Be date for each moraine.
[c] Sample WW11 not included in calculation as 3 σ beyond average.
[d] Sample WW14 not included in calculation as 3 σ beyond average.

Samples for TCN dating were collected from a small inset fan remnant (Fw3c, WW11–13), and from a faulted alluvial fan surface on the hanging wall of the thrust fault (Fw3a, WW14–16) and the footwall (Fw3b, WW17–21) that displaces the Fw3 surface. The soils have a moderately developed argillic horizon and iron oxy-hydroxides are abundant.

Alluvial fan surface Fw4 is inset into the older surfaces (Fig. 5B, E). The surface of alluvial fan Fw4 has numerous fresh meter-size boulders strewn across its surface and it is faulted in places. The surface has well defined bars and swales. Soils are poorly developed and organic matter-rich A and Cox horizons are not present, but there is an incipient calcic horizon forming a few decimeters below the surface similar to Stage III of Machette (1985). Samples for TCN dating were collected on this surface at the western end of the study area (Fw4, WW23 and WW25) and at the mouth of Whitewater River (Fw4, WW27, WW30 and WW31) where the alluvial

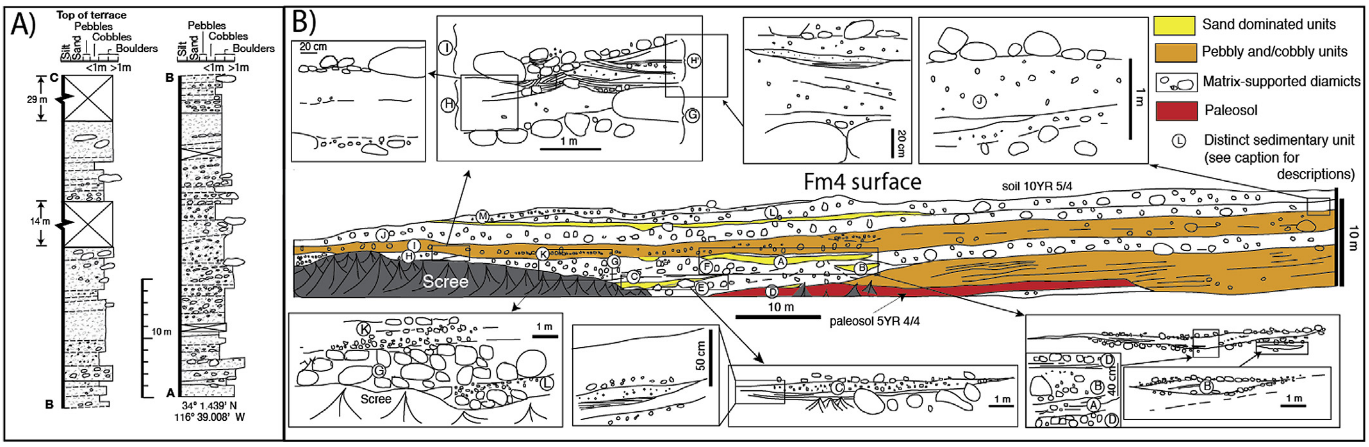

Fig. 4. Graphic sedimentary logs of an exposure in A) Fm1 (33°1.439′N/116°39.008′W) and B) an exposure through the Fm4 in the Mission Creek alluvial complex fan along the southern bank of the Mission Creek (33°59.784′N/116°35.834′W). See thick red lines in Fig. 2A for the locations. For part B) sedimentary units include: A – Crudely stratified pebbly (mm-size subrounded) sands; B – Massive cobbly pebbly sands; C – Low-angled cross-stratified channel fill sands overlain by massive pebbly (mm- to cm-size) sands; D – Cobbly pebbly sands with rare boulder. Unit is deeply weathered; E – Cobbly matrix supported diamicts; F – Massive matrix-supported bouldery cobbly diamict. Graduational upper contact; G – Bouldery matrix-supported cobbly diamict. Boulders reach 60–70 cm averaging 40 cm in a pebbly (mm-cm-size) coarse sand. Massive, though slight imbrication. Gradational upper contact; H – Crude undulating stratification with small channels (decimeter-size) pebbly fills near the top; cross-stratified mm- to cm-size pebbly sand are present towards the upper part of the unit; I – Pebbly sand, pebbles mm-cm size, with rare 3 cm-size pebbles, subangular to subrounded; J – Massive bouldery (decimeter-size) matrix-supported (pebbly sand) diamict with a relatively abrupt base; K – Crudely stratified cobbly pebbly unit; L – Massive matrix-supported bouldery diamict; M – Massive matrix-supported cobbly diamict with rare boulders.

fan is deformed by a thrust fault, displacing the surface by ~5 m (Fig. 2B).

The youngest alluvial fan surface, Fw5, is developed throughout the region, but this was not sampled for TCN dating. Abundant fresh boulders are present on this surface, and very distinct bars and channels are present. The soils are similar to those on alluvial fan surface Fw4. The historical and active alluvial fans in this study area are grouped together as the Fw6 and are characterized by abundant meter-size boulders, large bars and channels, and no soil development.

The sediments that comprise the alluvial fans in the Whitewater River study area are composed dominantly of meter-size beds of bouldery gravels that have crude sub-horizontal stratification and gradational bedding. Other beds comprise matrix-supported cobbles and pebbles, with graduation bedding gently inclined down valley. Fm1 and Fm2 deposits are particularly well exposed along the Whitewater River (Fig. 6).

5. Dating results

The results for the TCN dating are presented in Tables 1 and 2, and Figs. 7–9. Numerous workers have discussed problems associated with applying TCN methods to date alluvial fans, and discussions and summaries are provided in Matmon et al. (2006), Owen et al. (2011) and Blisniuk et al. (2012). In essence, however, two sets of factors contribute to the dating uncertainty. Firstly, problems are introduced in calculation of the production rate of TCNs, especially the uncertainty in correcting for variations in the geomagnetic field intensity. Table 1 presents our ^{10}Be TCN ages calculated using five different modeling schemes. Currently, there is no agreement on which scheme is the most appropriate to use. We favor the Lal (1991)/Stone (2000) time-dependent method, which incorporates a correction for variation in the geomagnetic field intensity. However, we recognize that ages calculated by other schemes differ by a few percent (with the exception of Lal (1991)/Stone (2000) time-independent method that is considerably larger) from the Lal (1991)/Stone (2000) time-dependent method. This difference does not effect the conclusions presented in the discussion.

As Owen et al. (2011) emphasized, geological factors introduce the second set of uncertainty. These include weathering, exhumation, prior exposure, and shielding of the surface by sediment and/or snow. With the exception of prior exposure, these factors generally reduce the concentration of TCNs in surfaces, which results in an underestimate of the true age of the landforms. Episodes of prior exposure result in an overestimate of the true age. Uneven distribution of these geological processes can produce a large spread in apparent exposure ages on a landform. Researchers commonly assess these effects by collecting multiple samples on a surface to examine the range of ages. If multiple surface samples possess similar apparent ages, the data suggest that the dated samples were not derived from older surfaces and/or were not weathered or exhumed. Since geologic processes acting on a surface are stochastic the spread of TCN ages on a particular surface would be large if geologic processes dominate.

Given these factors, we therefore collected multiple boulder samples on individual surfaces to help assess the geologic influences. In addition, TCN depth profiles can be used to help assess inheritance of sediment (Anderson et al., 1996; Hancock et al., 1999) and the likely erosion of the surface being dated (Hidy et al., 2010). Our depth profiles data suggest that we have an inheritance equivalent to about 6 ka and an erosion rate of about 4–5 m/Ma for the alluvial fan sediments (Table 1 and Fig. 7). This erosion rate refers to an alluvial fan surface that is generally moderately consolidated, but we could use this rate as a maximum estimate for

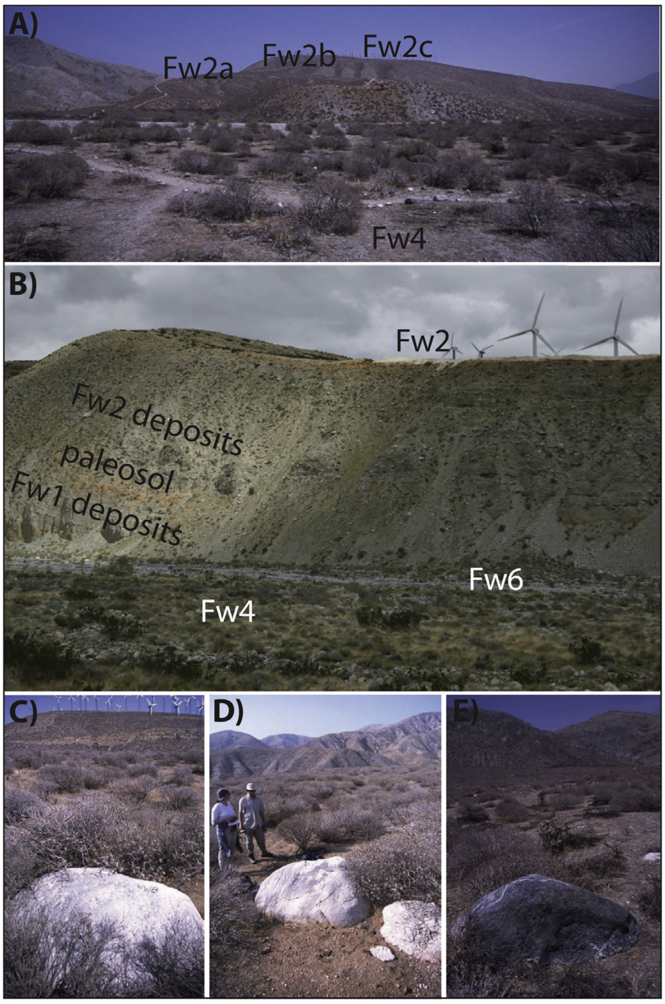

Fig. 5. Selected alluvial fans in the Whitewater River study area. A) View northeastward across alluvial fan Fw4 looking at alluvial fan surfaces Fw2a, Fw2b and Fw2c. B) View east across Whitewater River from alluvial fans Fw6 and Fw4 towards Fw2. Note the buried soil within the sediment fill of Fw2. Alluvial fans surfaces C) Fw2a showing sampled boulder WW8, D) Fw3c showing sampled boulder WW11, and E) Fw4a showing sampled boulder WW23.

boulder erosion. Applying an erosion rate of ~5 m/Ma to the boulders we dated would result in calculated TCN surface boulder ages of 10 ka being an underestimate of the true age by ~5%, an age of 50 ka by ~24%, and an age of 100 ka by ~50%. However, since we selected boulders that exhibited little signs of erosion and that often retained their original rounded depositional shapes, the effects of erosion are probably very much smaller and may even be negligible. Since we cannot determine the erosion history for each individual boulder we do not apply a correction for erosion to our boulder data. Similarly, since we cannot determine the prior exposure history of individual boulders that we sampled, we do not make a correction for inheritance for our boulder data. Furthermore, the prior exposure history of a boulder may be very different from the bulk sediment that was sampled in the depth profile analysis. However, we do recognize the possibility that boulders may have experienced prior exposure, and we consider the spread of boulder ages for surfaces in helping to assess this issue and the age of individual surfaces.

Given the geologic uncertainties associated with TCN ages, we summarize the ages for each surface in Table 2 listing the average boulder age (uncertainty = 1 σ) for each surface, the maximum age of a boulder on a surface, and the range of ages on a surface. If there is no prior exposure the maximum age of a boulder would be most likely to represent the closest age to the true age of surface abandonment/incision. On the basis of these data we assign a likely climatostratigraphic age to the surface, being very conservative with our estimate for the age. With the exception of samples collected from the surfaces in the upper reaches of Fm1 (samples MCF32 to MCF39) west of the Mission Creek, the populations of TCN ages on each surface tightly cluster. This provides confidence that the dating results do not suffer greatly from problems of weathering, exhumation and inheritance of TCNs in boulders that experienced prior exposure. The relatively larger age dispersion from samples MCF32 to MCF39 (surface FM1b) suggests that recent erosion had exhumed these samples. Plus samples MCF32 (11.7 ± 1.1 ka) and MCF36 to 39 (21.9 ± 2.3 ka, 32.9 ± 3.1 ka, 26.0 ± 2.3 ka, 38.2 ± 3.6 ka) exhibited significant signs of weathering (slight rounding as a result of granular disintegration and exfoliation), which may explain the younger ages. Given this, and the morphostratigraphic context, we expect the Fm1 surfaces to be older than the TCN ages suggest. Furthermore, the additional Fm1 surface to the east of the Mission Creek (Fm1c) on which samples MCF7–11 were collected has an age of 49.8 ± 6.6 ka, which is also younger than expected. McFadden (1982) suggested that our surface Fm1 is between 70 and 200 ka on the basis of soil development, and this is consistent with the extremely eroded topography of this surface. The overlapping ages of Fm1a and Fm1c with that for surfaces Fm2 and Fm4 (see below) is striking. However, the Fm1 surfaces are topographically and morphostratigraphically distinct and display a much greater degree of erosion than the Fm2 and Fm4 surfaces which are considered on this basis to represent younger surfaces. We therefore argue that Fm1 surface is older than marine isotope stage (MIS) 4 and may have even formed and subsequently have been abandoned/incised during an earlier glacial cycle.

The TCN age for Fm2, Fm4a and Fm4b are 66.5 ± 13.4 ka, 59.9 ± 9.1 ka and 63.0 ± 2.6 ka, respectively, which suggests that these surfaces formed during MIS 4. Our TCN depth profile for Fm2 has an age of $48.7^{+16.9}/_{-11.9}$ ka. This also supports the view that Fm2 surface was formed and subsequently abandoned during MIS 4 (given the large uncertainty), and it is considered likely that Fm3 and Fm4 were also abandoned during MIS 4. Furthermore, McFadden (1982) on the basis of soil development suggested that the soils on our Fm2 surface formed sometime between 13 and 70 ka.

Fw2 and Fw3 surfaces in the Whitewater River study area have ages that are similar to Fm2, Fm3 and Fm4. These include on Fw2 (a, b, c) surfaces of 57.1 ± 9.7 ka, 61.0 ± 22.7 ka and 54.5 ± 13.1 ka based

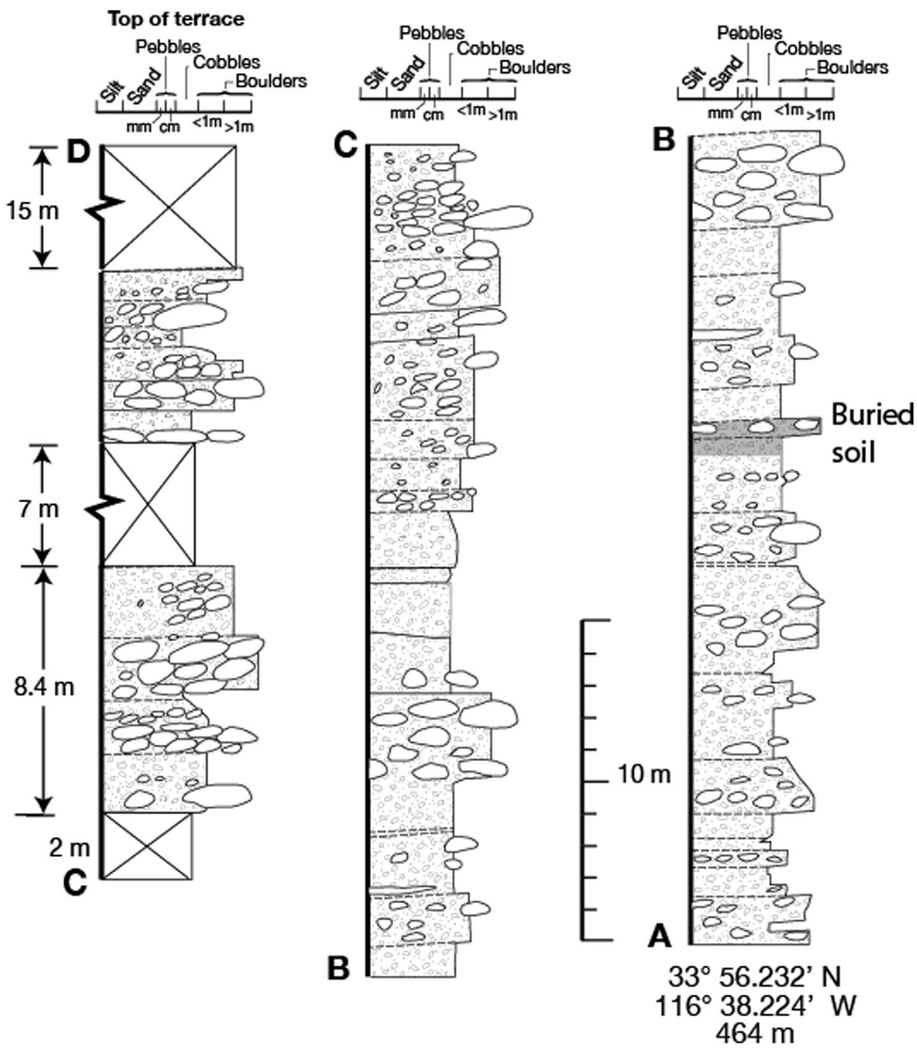

Fig. 6. Graphic sedimentary log for the sediments within the main Whitewater River alluvial fan along the eastern side of Whitewater River at the location shown in Figs. 2B and 5B. Note the position of the buried soil that marks the junction between sediments of the Fw1 and Fw2 alluvial fan sediments.

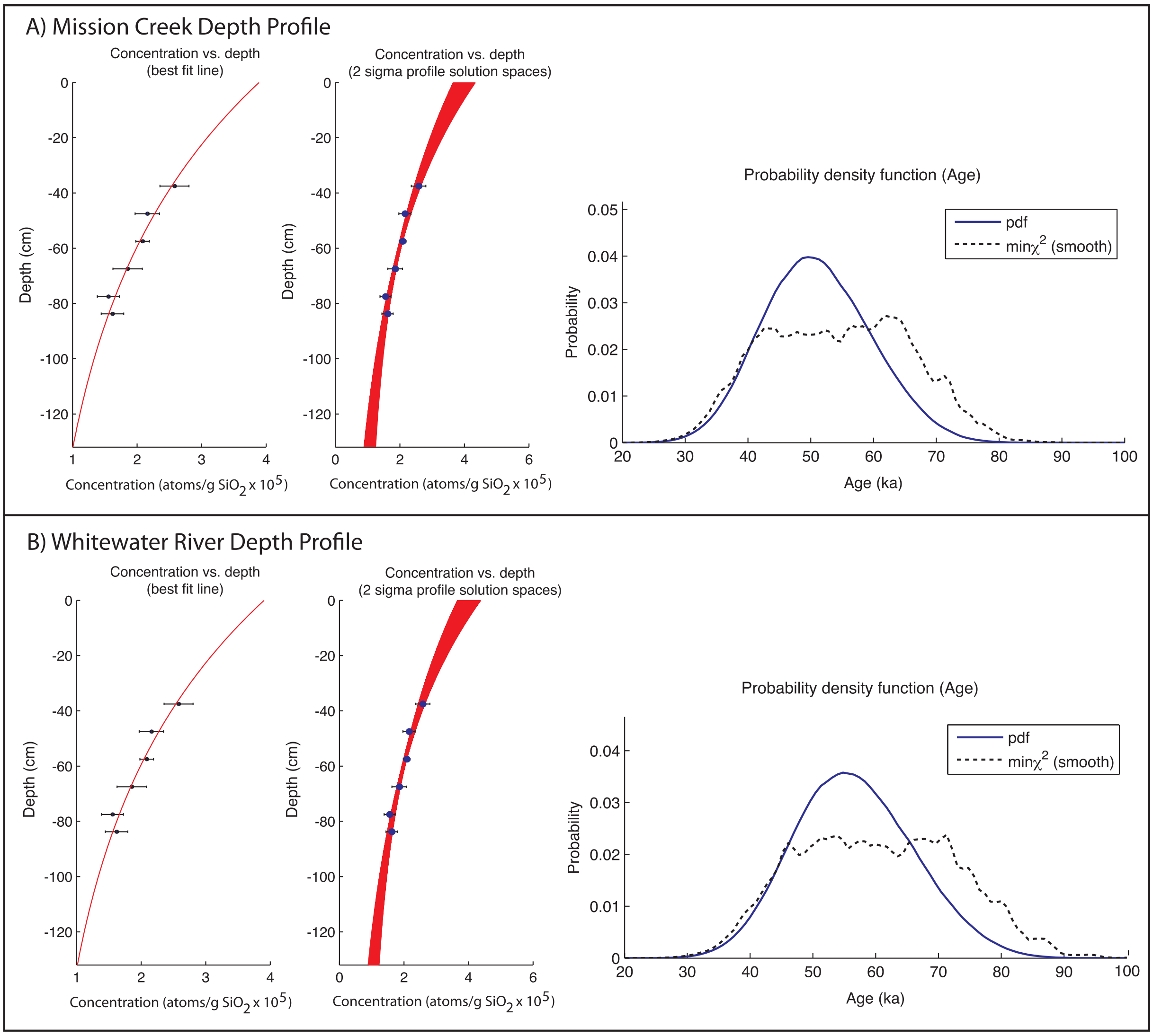

Fig. 7. Concentration versus depth plots illustrating the 2 σ profile solution spaces (middle) and best fits (left) and results of 2 sigma age solution spaces (right) for A) Mission Creek and B) Whitewater River pits determined using the methods of Hidy et al. (2010).

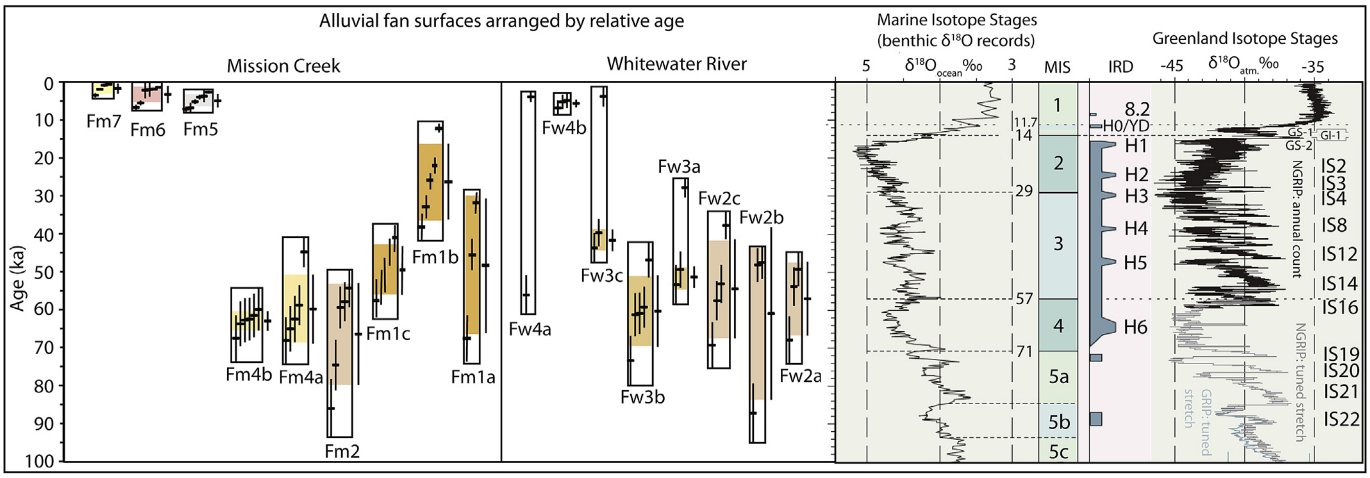

Fig. 8. Plots of ^{10}Be ages against relative ages of alluvial fan surfaces. The thin black lines within the boxes are individual ^{10}Be ages for boulder on each surface and the lines outside the boxes and the gray shading within the boxes represent the mean and 1 s uncertainty.

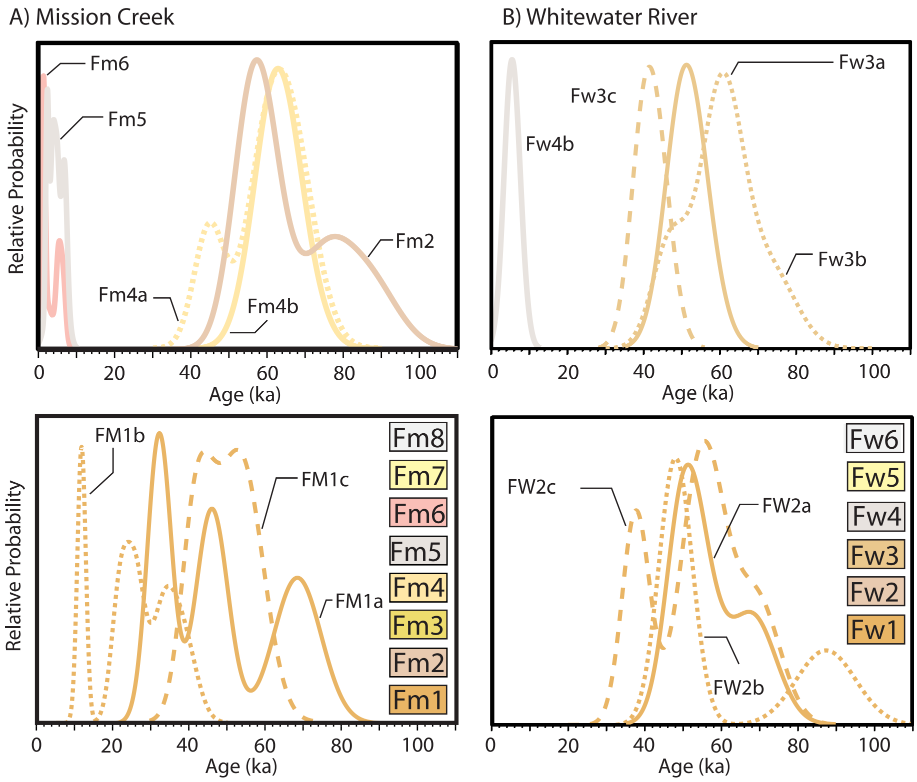

Fig. 9. Relative probability plots for ^{10}Be TCN exposure ages from surface boulders on A) Mission Creek and B) Whitewater River alluvial fan complexes. The surfaces are arranged by relative age based on morphostratigraphy. These are compared with the marine and Greenland isotope stages, and Heinrich events (from Cohen and Gibbard, 2011 and references cited within).

on boulder ages and a depth profile age of $53.9^{+19.0}/_{-13.0}$ ka, showing that they were likely abandoned during MIS 4. Fw3 has similar ages that are 51.4 ± 2.8 ka (Fw3a) and 60.4 ± 9.4 ka (Fw3b), although Fw3c has an age of 41.7 ± 2.8 ka, but the ages range from 37.8 to 69.4 ka for this surface.

Both the Whitewater River and the Mission Creek study areas have younger alluvial fans, which have Holocene ages. For the Mission Creek alluvial fan complex these include Fm5 (4.9 ± 1.8 ka), Fm6 (3.3 ± 2.3 ka) and Fm7 (1.7 ± 1.3 ka). The only well-dated younger surface in the Whitewater River study is Fw4b, which has an age of 5.6 ± 1.1 ka. Two boulders were sampled on Fw4a, one with an age of ~3.9 ka and the other ~56 ka. The older age likely represents a boulder that had previously exposure to cosmic rays. Given the potential for inherited TCNs, we are reluctant to assign the surfaces to a particular time within the Holocene. However, it is noted that many of the TCN ages are considerably younger than 6 ka (the value of inheritance determined on sediment in our depth profiles) and hence inherited TCNs in boulders is likely to be small. The poorly developed soils, fresh surface features and morphostratigraphic position and context support the views that these alluvial fan surfaces were abandoned during the Holocene.

In summary, the alluvial fan surfaces in the study areas were abandoned/incised during three key periods. The oldest old alluvial fan surfaces or buried fans (Fm1 and Fw1) were likely formed and subsequently abandoned significantly before MIS 4 and might have been abandoned during an earlier glacial cycle. The second set is a series of alluvial fans that date to MIS 4 (Fm2, Fm3, Fm4, Fw2 and Fw3), and the third set date to the Holocene (Fm5, Fm6, Fm7, Fw4, Fw5 and Fw6). Table 3 summarizes these surfaces and shows the correlation of each between the two detailed study areas.

6. Discussion

The alluvial fans within and around our detailed study areas provide a potentially very important archive that can be used to determine the nature of sediment transfer, tectonics and climate change. The sedimentology and geomorphology of the alluvial fans show that they formed as a consequence of high magnitude-low frequency large debris and/or hyperconcentrated flows, and with intermittent stream flows. For further discussion of depositional processes that produce bouldery diamictons in alluvial fans we refer the reader to the comprehensive discussion in Barnard et al. (2006).

Three distinct phases of alluvial fan development are evident from the geomorphology of the study areas (Fig. 10). Firstly there is a distinct phase of alluvial fan aggradation that produces the Fm1 alluvial fan and Fw1 fanglomerates in the Mission Creek and Whitewater River study areas. This resulted in the development of a valley fill throughout the Whitewater River valley and the ESE directed Fm1 alluvial fan that is now beheaded at the eastern end of the Mission Creek study area. The morphology of the Fm1 alluvial fan shows that it is clearly sourced from the upper Whitewater River and much of the main drainage of the Whitewater River may have been along what is now the Mission Creek drainage at the Mission Creek alluvial fan complex.

Next there was a time during which the Whitewater River entrenched northward, resulting in the beheading and abandonment of the Fm1 alluvial fan. Likely contemporary with this, Mission Creek incised into the beheaded alluvial fan Fm1. There followed a period of relative landscape stabilization allowing a soil to develop on Fm1 and Fw1 deposits, which is now apparent in sections along the Mission Creek and Whitewater River drainages

(Figs. 4, 5B and 6). Fm2 and Fw2 alluvial fan surfaces date to MIS 4, so the age of Fw1 and Fm1 alluvial fan aggradation must be considerably older than MIS 4 to allow for enough time for soil development. Given the distinct soil development of the buried soil (with much greater clay content than that for Fw2 surfaces) it is likely that it took many tens of thousands of years to develop, and we argue that this soil likely formed in an earlier glacial cycle.

The second phase of alluvial fan development resulted in extensive alluvial fan aggradation with the Fw2 alluvial fan building out down the lower Whitewater River valley burying Fw1 deposits (and its soil) to form a distinct alluvial fan succession. At the same time the Mission Creek alluvial fan Fm2 developed burying Fm1 (together with its soil Fig. 5B) in the lower reaches of Mission Creek. This was rapidly followed by the progressive incision and cannibalization of the alluvial fan Fm2 controlled by Mission Creek to produce alluvial fan surfaces Fm3 and Fm4. In the Whitewater River study area, Fw2 was cannibalized to produce Fw3. Our TCN ages on Fm2 and Fw2 show that the surfaces were abandoned during MIS 4. Since these ages effectively represent the final stages of deposition and incision of the alluvial fan, we can infer that the surfaces were abandoned/cannibalized during MIS 4. The similar ages for Fm4 (and Fm3, constrained by Fm2 and Fm4) and Fw3, suggest the cannibalization was rapid and that MIS 4 was a time of major and rapid landscape readjustment as alluvial fans were incised and resedimented. As mentioned above, we argue that inheritance of TCN from prior exposed boulders is small given the young Holocene ages we have in the youngest alluvial fans, and our depth profiles show that inheritance is likely only a few thousand years for sediment.

A period of quiescence in terms of alluvial fan formation followed the formation of Fm3, Fm4 and Fw3 alluvial fans until the Holocene when the third phases of alluvial fan development began. The Holocene is marked by the formation and abandonment of several alluvial fan surfaces, including Fm5, Fm6, Fm7, Fw4 and Fw5. Alluvial fans are still forming today, represented by the active alluvial fan surfaces Fm8 and Fw6.

Active faults deform some of the alluvial fan surfaces in the Whitewater River study area. Alluvial fan surface Fw3 (Fw3a and Fw3b), for example, is displaced by a thrust fault by at least 100 m. In addition, the dextral-slip Banning fault displaces alluvial fan surface Fw2. Yule and Sieh (2003), however, suggest a maximum 4 km offset of the Fw2 surface. However, it is not possible to define any offset landform to determine the amount of displacement along the Banning fault. An active anticline also traverses Fw2 and the NE trending scarps, which are likely fault scarps, stress the influence of tectonics on alluvial fan development in this region. More detailed examination of the faulting awaits further study.

None of the alluvial surfaces in the Mission Creek alluvial fan complex are offset by the Mission Creek fault. The Mission Creek channel traverses the Mission Creek fault (Fig. 2A) unhindered suggesting that there appears to have been no motion along the Mission Creek fault since MIS 4. If the Mission Creek fault had moved since the initial incision of the Mission Creek through the alluvial fan complex then there would probably be evidence of right-lateral offset preserved in differential erosion of the Mission Creek cliffs through Fm1, Fm2 and Fm3. As such, significant erosion and enlargement of the westward cliffs of the Mission Creek would be apparent to the south of the Mission Creek fault. We do not see such evidence and therefore we suggest that any slip along this stretch of the Mission Creek fault has been small since at least MIS 4.

Clearly our TCN ages define two periods of alluvial fan development/incision in the late Quaternary during: (1) MIS 4, and (2) the Holocene. We cannot attribute a paraglacial influence on alluvial fan formation in our study area because there is no evidence of any significant glaciation, and hence glacial influences, in the San Bernardino mountains prior to the Last Glacial Maximum (~18–24 ka), although there were very minor Late Glacial and early Holocene advances on San Gorgonio (Owen et al., 2003). Although there is a tectonic influence on the Whitewater River alluvial fan complex and there is an autocyclic influence on sedimentation, the two distinct periods of alluvial fan development suggest a climatic influence that might reflect a regional climatic signal. To test whether this is the case we have compiled studies of Late Quaternary alluvial fans in the American Southwest that have applied numerical dating methods. These are summarized in Table 4 and Fig. 11.

TCN dating is the most commonly used method to define alluvial fan ages in the American Southwest, but other methods include optically stimulated luminescence (OSL), thermoluminescence (TL), radiocarbon, U-series dating, and tephrochronology. Each of these dating methods has their own problems and limitations; and hence the uncertainty in defining the ages of alluvial fan formation is quite high (often many millennia to tens of millennia). Furthermore, each dating method dates a different aspect of the formation of an alluvial fan, for example, times of aggradation/incision/surface abandonment. OSL, TL and radiocarbon dating, for example, generally date the timing of alluvial fan sedimentation, whereas U-series and TCN dating generally provide minimum ages on alluvial fan formation and/or timing of abandonment of an alluvial fan surface. Tephrochronology can provide an event stratigraphy for the alluvial fans. As a consequence of the large uncertainty associated with most of the dating methods and the differences stage that is being dated it is difficult to correlate alluvial fans across a large area, and often even within a region. Nevertheless, several generalizations can be made based on our compilation.

The compilation of data firstly suggests that the pattern of alluvial fan formation in the American Southwest is complex. Spelz et al. (2008), for example, note that alluvial fan ages in the American Southwest cluster at numerous times through the Late Quaternary and earlier. These include: modern to ~2 ka; ~2 ka to ~4 ka; ~4 to ~8.7 ka; ~9 to ~17 ka; ~16 to ~39 ka; ~60 to ~86 ka; ~124 to ~129 ka; and ~240 to 730 ka. Clearly there is some overlap between ages of some clusters, which may reflect the large uncertainty associated with the dating. Spelz et al. (2008) suggested that this clustering of ages reflects climate modulated alluvial fan formation. Of particular note with these studies, and especially with our new data is that they indicate a general major phase of alluvial fan formation during the early part of the Last Glacial and abandonment/incision of alluvial fans during MIS 4, followed by a stage of alluvial fan formation during the Holocene. There are, however, study areas where alluvial fans have formed during late MIS 3 and MIS 2, such as Baja California, Southern Transverse Ranges and Owens Valley. Some of these regions such as in Owens Valley have been strongly influence by oscillating glaciers and the alluvial fans are paraglacial in origin, but of course these

Table 3
Correlation of alluvial fan surfaces between the Mission Creek and Whitewater River alluvial fan complexes.

Mission creek alluvial fan complex	Whitewater alluvial fan complex	Assigned ages
Fm7	Fw6	Historical/active
Fm6	Fw5	Middle to late Holocene
Fm5	Fw4a, b	Middle to late Holocene
Fm4b, a	Fw3a, b, c	Late MIS 4
Fw3		Late MIS 4
Fm2a, b, c	Fw2a, b, c	Late MIS 4
Fm1a, b, c	Fw1	>MIS 4

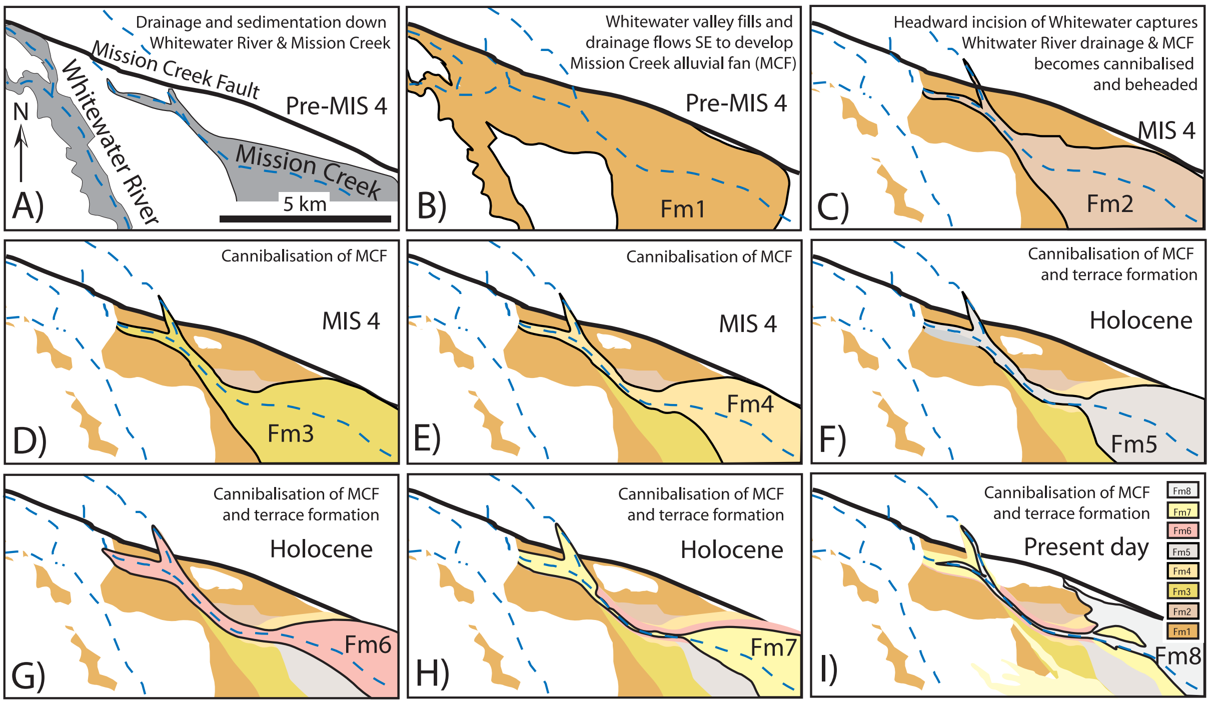

Fig. 10. Schematic reconstruction of the evolution of the Mission Creek in relation to the Whitewater River drainage system.

alluvial fans are confined to locations where the catchments were glaciated (e.g. Benn et al., 2006).

In an attempt to compare our ages directly with other studies that utilize ^{10}Be TCN surface exposure dating, we compile all the ^{10}Be ages for the American Southwest (Table DS1). All the ages are recalculated using the Lal (1991)/Stone (2000) time-dependent model and a zero-erosion assumption to be directly comparable with our new ages. These data are then plotted as a normal kernal density estimate (NKDE) using the camelplot MATLAB code by Balco (http://depts.washington.edu/cosmolab/pubs/gb_pubs/camelplot.m: Fig. 12). Readers are referred to Lowell (1995) for a basic discussion of the NKDE diagram concept. The NKDE plots allow us to assess the clustering of ^{10}Be ages through time. We are aware of the limitation of this technique, which compares all data disregarding the fact that some ages may be considerably older or younger than the true age of the surface abandonment (as discussed in detail above). However, given the large data set (380 ^{10}Be ages) the NKDE plots allow some generalizations to be made about regional correlations assuming that outlying ages are subsumed in the general pattern. The probability distributions presented in Fig. 12 show increased clustering with decreasing age. This likely reflects a preservation bias as a greater number of suitable boulders are available for younger surfaces and thus larger datasets are available. Five dominant peaks are apparent, two in MIS 1 and one in each of MIS 2, MIS 3 and MIS 4, which suggests that fan development and abandonment occurs on a Milankovitch timescale frequency. The peaks in MIS 1 and MIS 4 support our view of fan surface abandonment in the Mission Creek and Whitewater River areas. However, Fig. 12 also indicates abandonment of alluvial fan surfaces elsewhere in the American Southwest during late MIS 3 and 4. It must be remembered that the data pooled in this plot is sourced from all alluvial fans in the region, including some paraglacial fans that may have responded differently to the majority of alluvial fans throughout the region and could explain the peaks in MIS 2 and MIS 3. Moreover, individual studies with very large datasets would also bias the plots. The key point, however, is that this compilation helps illustrate the complexity of the alluvial fan record in the American Southwest and their potential to derive important geologic data.

Numerous researchers have proposed process-response models for aggradation associated with catchments in desert environments, with some arguing that fan aggradation is associated with a relative increase in aridity (e.g., Bull, 1977, 1991, 2000; Wells et al., 1987, 1990), whereas others interpret fan aggradation as occurring with a relative increase in rainfall (e.g., Ponti, 1985; Harvey et al., 1999a,b). The arid model of alluvial fan formation is widely accepted for the American Southwest and it proposes that aggradation of alluvial fans coincides with transitions from glacial to interglacial cycles when the balance of stream power and sediment supply passed critical geomorphic thresholds (Bull, 1977, 1991, 2000). This occurs due to reduced annual rainfall and increased temperatures that lead to decreased soil moisture and vegetation density, which reduces infiltration rates and exposes soil to erosion. This in turn leads to increased sediment supply and triggers valley floor aggradation. The aggradation event continues until a deposition–erosion threshold is crossed and sediment concentration decreases due to either the removal of hillslope colluvium and/or the stabilization of the colluvium produced by a higher vegetation cover on hillslopes. At this point the geomorphic system becomes transport limited and fluvial systems will begin to incise through the alluvial surface and develop an erosional strath upon which the next alluvial fan in the telescopic sequence will be deposited.

As Spelz et al. (2008) highlights, according to the arid alluvial fan model the alluvial fan sediments should have interglacial/interstadial ages and their abandoned surfaces can form at anytime thereafter when the deposition-erosion threshold is crossed, but the age of surface abandonment should be older than the onset of the next glacial/stadial period when rainfall and runoff increase dramatically. This model suggests that alternating cycles of erosion

Table 4
Studies of Late Quaternary alluvial fans in the America Southwest that have been dated using numerical methods, summarizing ages, nomenclature and methods.

Study areas	Name of surface[a]	Age[b,c]	Method used to determine age	Reference for study
Yucca Mountain, NV	Q2c	55 ± 20 ka	Uranium-series dating	Rosholt et al. (1985)
Death Valley				
Black Mountains, southern Death Valley	Q3b	4–7 ka	OSL dating	Sohn et al. (2007)
	Q3a	11–17 ka		
	Q2d	25 ka		
Western side of southern Death Valley	Qai	100–40 ka, mean ~70 ka	^{36}Cl TCN dating	Machette et al. (2008)
	Qao	~170 ka		
Northern Death Valley	Q4b	0.14–0.30 ka	^{14}C dating	Klinger (2001a, b)
	Q4a	<1.2 ka	Tephrochronology	
	Q3a	<12 ka	Soil Development	
	Q2	30–180 ka	Soil Development	
	Red Wall Canyon (Q2c)	63 ± 8 ka to 70 + 22/−20 ka	^{36}Cl and ^{10}Be TCN dating	Frankel et al. (2007a)
	Indian Creek (Qfiy)	71 ± 8 ka	^{10}Be TCN dating	Frankel et al. (2007b)
	Furnace Creek (Qfio)	94 ± 11 ka		
	Perry Aiken Creek	71 ± 8 ka	^{10}Be TCN dating	Ganev et al. (2010)
	Indian Creek (Qfl)	6 ± 2 ka	^{10}Be TCN dating	Frankel et al. (2011)
	South Mud Canyon (Q3a)	17 ± 2 ka		
	Cucomongo Canyon (Qfi)	39 ± 3 ka		
	Q4b	2.0–92.6 ka; 24.4 ± 27.2 ka	^{10}Be TCN dating	Owen et al. (2011)
	Q4a	1.8–88.0 ka; 24.6 ± 28.5 ka		
	Q3b	4.0–57.1 ka; 18.3 ± 18.8 ka		
	Q3a	7.6–152.6 ka; 68.6 ± 35.4 ka		
	Q2c	41.3–235.5 ka; 87.8 ± 43.8 ka		
	Q2b	27.3–191.1 ka; 68.6 ± 58.5 ka		
Leidy Creek Fan	Qfcl,Qfcm, Qfce, Qfl	11–0 ka >100–50 ka	^{14}C dating, tephra, TL and ^{10}Be dating & tephrochronology	Reheis et al. (1996)
Owens Valley				
Fish Creek Springs	South fan	7.1, 3.2, 1.5 ka	^{10}Be and ^{26}Al TCN dating	Zehfuss et al. (2001)
	North fan B	8.1 ± 1.9 ka		
	North fan A	13.2 ± 1.0 ka		
	North fan C	14.5 ± 0.9 ka		
Blairs, Shepherd and Symmes Creeks	Qf4	4.1 ± 1.0 ka	^{10}Be TCN dating	Le et al. (2007)
	Qf3c	4.4 ± 1.1 ka		
	Qf3a	25.8 ± 7.5 ka		
	Qf2b	60.9 ± 6.6 ka		
	Qf1	123.7 ± 16.6 ka		
Symmes Creek	F	3–8 ka	^{10}Be TCN dating	Duhnforth et al. (2007)
Shepherd Creek	D&E	3–11 ka		
	C	15–33 ka		
	A&B	86–74 ka		
Lone Pine fan	Faulted fan	11.6 ± 3.7 ka and 11.7 ± 3.6 ka	^{10}Be and ^{26}Al TCN dating	Bierman et al. (1995)
	Qg4	1.2 ± 0.3 ka and 2.0 ± 1.0 ka		
	Qg3	25.4 ± 6.0 ka and 24.0 ± 5.3 ka		
	Qg1	98.2 ± 30.1 ka and 67.3 ± 18.8 ka		
Lone Pine and Tuttle fans	not named	9–13 ka	^{10}Be TCN dating	Benn et al. (2006)
	not named	16–18 ka		
	Qg3	23–32 ka		
	not named	32–44 ka		
	Qg1	80–86 ka		
Mojave Desert				
Little Rock Creek, Western Mojave	Fan 0	16 ± 5 ka	^{10}Be and ^{26}Al TCN dating and calibrated fault slip	Matmon et al. (2005, 2006)
	Fan 1	29 ± 7 ka		
Mojave desert/Lower Colorado River	Q4b	Modern	Active channels	Bull (1991, 2007)
	Q4a	0.1–2 ka	Morphological criteria	
	Q3c	2–4 ka	Morphological criteria	
	Q3b	~8 ka	^{14}C dating	
	Q3a	~12 ka	^{14}C dating	
	Q2c	~60 ka	^{230}Th/^{234}U, ^{10}Be TCN dating	
	Q2b	~125 ka	^{230}Th/^{234}U dating	
	Q2a	~240–730 ka	K/Ar dating	
	Q1	>1200 ka	K/Ar dating	
Vidal Valley, Lower Colorado River region	Q3b	>6 ± 1 ka	^{230}Th/^{234}U dating	Ku et al. (1979)
	Q2c	>61 ± 5 ka		
	Q2b	>83 ± 10 ka		
Silver Lake	Qf3	>3.4 & <8 ka	^{14}C dating	Wells et al. (1987, 1987)
	Q3b	<8.7 ka		
	Q3a	>9.5 and <11.8 ka		
Zzyzx, Lake Mojave	Group 3 fans	<8.5 ka	Lake stratigraphy	Harvey et al. (1999b)
	Group 2 fans	(13–10.5) – 8.5 ka		
	Group 1 fans	>(18.5 – 13) ka		

(continued on next page)

Table 4 (*continued*)

Study areas	Name of surface[a]	Age[b,c]	Method used to determine age	Reference for study
Kyle Canyon, near Los Vegas Valley, Nevada	Q2c	75 ± 20 ka	$^{230}Th/^{234}U$ dating	Sowers et al. (1989)
	Q2b	129 ± 6 ka		
South side of Transverse Ranges				
Cajon Pass, CA	Q2c	55 ± 8 ka	Calibrated fault slip	Weldon and Sieh (1985)
Plung Creek	Qow3b	~32–36 ka	^{14}C dating	McGill et al. (2013)
	Qyf2	10.2–10.6 ka	^{14}C and OSL dating	
Briska Palms	T2	35.5 ± 2.5 ka	^{10}Be TCN dating	van der Woerd et al. (2006)
Briska Palms	T2	>45.1 ± 0.6 ka	U-series	Fletcher et al. (2010); Behr et al. (2010)
	T2	50 ± 5 ka	^{10}Be TCN dating	
Peninsula Ranges				
Santa Rosa Mountains	Q3b	6.1 ± 0.6 ka and 4.7 ± 1.5 ka	U-series and ^{10}Be dating	Blisniuk et al. (2012)
	Q2c	35 ± 7 ka	^{10}Be TCN dating	
	Q2c	33.6 ± 0.9 ka and 41.1 ± 6.5 ka	U-series and ^{10}Be dating	
Coyote Mts./Elsinore fault	Q2c	41.4 ± 1.6 ka and 46.3 ± 8.5/43.1 ± 3.3 ka	U-series and ^{10}Be dating	Blisniuk et al. (2012)
Ash Wash	Q3b	5.2 ± 0.3 ka and 2.1 ± 1.0 ka	U-series and ^{10}Be dating	Blisniuk et al. (2012)
Fig Tree Valley	q3b	6.0 ± 1.0 ka and 3.9 ± 2.8 ka	U-series and ^{10}Be dating	Blisniuk et al. (2012)
Baja California				
Western Sierra el Mayor	Q4	15.5 ± 2.2 ka	^{10}Be TCN dating	Spelz et al. (2008)
	Q7	204 ± 11 ka		
Eastern Sierra el Mayor	Qt1-Qt4	17–31 ka	^{10}Be TCN and OSL dating	Armstrong et al. (2010)

Nb. many of the early studies do not provide sufficient data to recalculate the ages.
[a] Nomenclature used in original publication.
[b] Ages in original publication.
[c] Published ages in our comparison, recalculating them using current production rates would change the ages by a few percent, although this would be hidden by the geological uncertainty.

and aggradation take place over relatively long time periods that correspond with the glacial and interglacial cycles, respectively.

Clearly under this arid alluvial fan model we would expect alluvial fan aggradation to occur during the Pleistocene–Holocene transition in the America Southwest as the climate changed from cool and wet to warm and dry. Miller et al. (2010) provided data to support periods of alluvial fan aggradation across the Mojave Desert at 9–14 ka, which was a time of long transition to a warm and dry climate. Moreover, Miller et al. (2010) also showed that alluvial fan aggradation occurred at between 3 and 6 ka in the Mojave Desert, which was also a cool and wet time. Miller et al. (2010) highlighted that these phases of alluvial fan formation largely correlate with times of increased sea-surface temperatures in the Gulf of California and enhanced warm-season monsoons. This correlation suggests that sustained alluvial fan aggradation may be driven by intense summer-season storms, and that the close proximity of the Mojave Desert to the Pacific Ocean and the Gulf of California promotes a partitioning of landscape-process responses to climate forcing that vary with seasonality of the dominant storms. Miller et al. (2010) also suggested that cool season Pacific frontal storms cause river flow, ephemeral lakes, and alluvial fan incision, whereas periods of intense warm-season storms cause hillslope erosion and alluvial fan aggradation.

Under the arid alluvial fan model, we would expect alluvial fans to begin to form at the transition from the cooler and wetter MIS 4 stadial to the warmer and drier MIS-3 interstadial. However, our study and numerous others suggest that alluvial fan abandonment took place during MIS 4. From Miller et al. (2012) it is clear that correlating alluvial fans with climatostratigraphic times is challenging. This challenge is even greater for Pleistocene alluvial fans because of the larger dating uncertainties associated with older landforms. We recognize that the large uncertainty in our MIS 4 ages does not allow us to adequately test whether our alluvial fans, and those in other areas of the American Southwest that have similar ages, fully comply with the arid alluvial fan model. But it highlights there is still much to be known about what conditions favor alluvial fan formation during the Late Quaternary and earlier.

In essence, the formation of alluvial fans in our study area, and mostly likely throughout the American Southwest is controlled dominantly by climate modulated sediment supply. However, other factors, such as changing stream directions (e.g. re-routing of the Whitewater River from across the Mission Creek region that produced alluvial fan Fm1) and tectonics influence alluvial fan formation. Correlating alluvial fans across the American Southwest is challenging and as such makes climatostratigraphic correlations and causal factors difficult to determine. Our study also highlights a potential limitation to TCN exposure dating. The Mission Creek succession clearly shows younger ages on alluvial fan surfaces that are morphostratigraphically older than well-dated surfaces of MIS 4. These results suggest that boulder erosion and alluvial fan surface denudation potentially limit the use of surface exposure dating in this setting to deposits younger than ~70 ka, highlighting the need for careful field geomorphic and sedimentological evaluation in combination with TCN sampling.

7. Conclusions

The Mission Creek and Whitewater River alluvial fan complexes comprise dominantly bouldery debris deposits with surfaces dating to early in the Last Glacial or more likely the penultimate glacial cycle, MIS 4, and the Holocene. The lack of alluvial fan ages during the latter part of the Last Glacial (MIS 2 and 3) suggests that there has been little alluvial fan formation/erosion during that time in our study areas. The oldest alluvial fan surfaces in the Mission Creek region were beheaded by the Whitewater River drainage, indicating that the oldest alluvial fans in the Mission Creek region underwent significant capture/rerouting by the Whitewater River drainage. Our new data, and those for other alluvial fans throughout the American Southwest, help support the view that there is a strong climatic control on alluvial fan formation in this region. Attributing

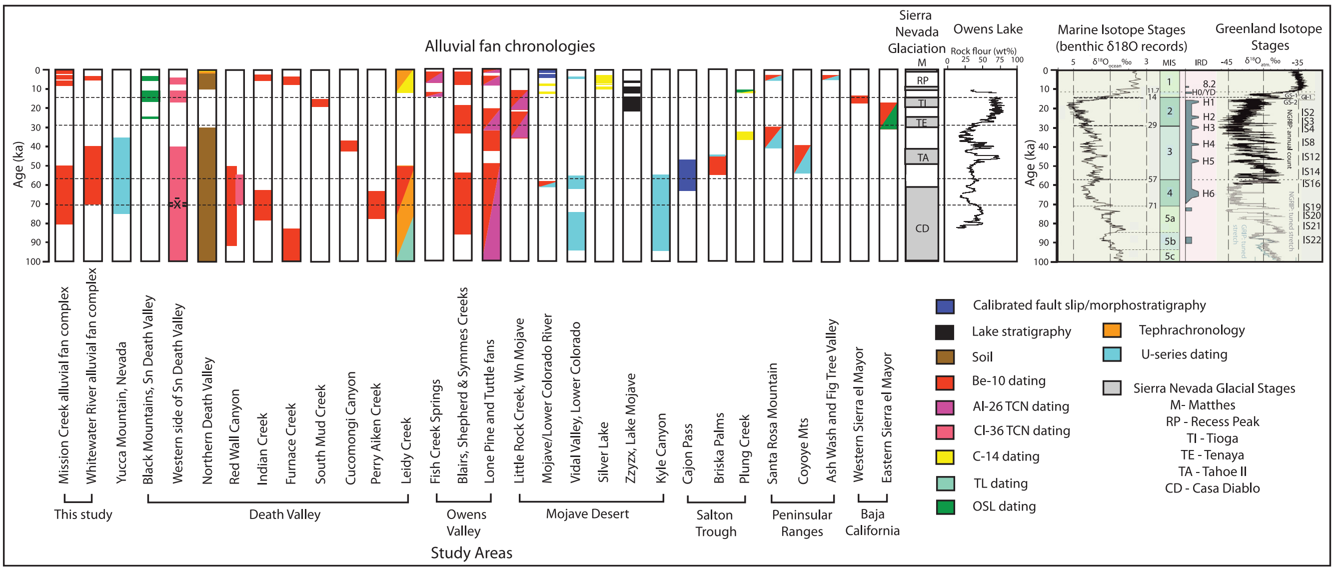

Fig. 11. Schematic representation of alluvial fan ages for study areas in the America Southwest compared with Sierra Nevada glaciation (from Gillespie and Clark, 2011), Owens Lake glacial silt record (from Bischoff and Cummins, 2001), marine and Greenland isotope stages, and Heinrich events (from Cohen and Gibbard, 2011 and references cited within). Alluvial fan data from Ku et al. (1979), Rosholt et al. (1985), Weldon and Sieh (1985), Wells et al. (1987), Sowers et al. (1989), Bull (1991, 2007), Beirman et al. (1995), Reheis et al. (1996), van der Woerd et al. (1996), Harvey et al. (1999), Klinger (2001a, b), Matmon et al. (2005, 2006), Benn et al. (2006), Dühnforth et al. (2007), Frankel et al. (2007a, b, 2011), Le et al. (2007), Sohn et al. (2007), Machette et al. (2008), Spelz et al. (2008), Armstrong et al. (2010), Behr et al. (2010), Blisniuk et al. (2010, 2012), Fletcher et al. (2010), Ganev et al. (2010), McGill et al. (2013). See Table 3 for more details on each alluvial fan study.

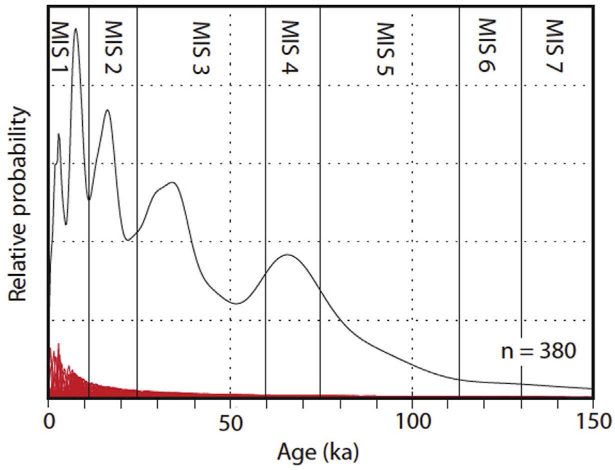

Fig. 12. Synthetic probability plot for all ^{10}Be ages on surface boulders in the semi-arid American Southwest. MIS = marine isotope stages after Martinson et al. (1987).

alluvial fan formation to particular climatostratigraphic times is challenging and dating uncertainties prevent us from definitively determining what the climatic and geomorphic conditions and/or thresholds are for alluvial fan formation in our study areas. However, having abundant alluvial fan ages that fall into MIS 4—a wet and cool time—suggests that the arid alluvial fan model proposed by numerous workers (e.g. Bull, 1977, 1991, 2000; Wells et al., 1987, 1990) might not be fully valid. Moreover, as Miller et al. (2010) showed, alluvial fan formation during wet and cool times in the Holocene also suggests that alluvial fan formation is not in phase with what is hypothesized in the arid alluvial fan model. However, more precise dating of alluvial fans is required to fully test this suggestion.

Active thrust and strike-slip faults deformed alluvial fan surfaces in the Whitewater River study area highlighting the influence of tectonics on the alluvial fan development in this region. Slip rates, however, cannot be adequately defined because distinct landforms cannot be identified and used as pinning points across faults. Since MIS 4, Mission Creek has maintained a consistent channel that is entrenched within the Mission Creek alluvial fan complex and traverses the Mission Creek fault. The lack of any displacement of this drainage, especially its consistent course that produced Fm2 and Fm3 surfaces, indicates that there may have not been no motion along the Mission Creek Fault since MIS 4. Our TCN ages on alluvial fans in this region will help in future tectonic geomorphic studies.

In summary, alluvial fans in our study provide a record of climate modulated sediment transfer and erosion, and are deformed and displaced in places by active faults. Furthermore, they help illustrate the complex autocyclic and allocyclic controls on alluvial fan development in tectonically active settings such as southern California and other tectonically active regions.

Acknowledgments

Many thanks to two anonymous reviewers and Kimberly Blisniuk for their very constructive and useful comments on our manuscript. The TCN work was performed under the auspices of the U. S. Department of Energy by the University of California, Lawrence Livermore National Laboratory under Contract No. W-7405-Eng-48 as part of an IGPP/LLNL research grant. John Matti and Doug Morton for introducing us to the field area and for discussions throughout the duration of this project. Sincerely thanks to Karen Goodall who helped collect and processed the WW samples. SJC thanks the USGS and UK Quaternary Research Association for helping to provide financial support to help undertake the fieldwork component of this research. Any of the statements, or comments, made in this scientific paper should be regarded as personal and not those of the Welsh Government, any constituent part or connected body. Kate Hedrick and Jenny Arkle for their careful and constructive comments on our manuscript.

Appendix A. Supplementary data

Supplementary data related to this article can be found at http://dx.doi.org/10.1016/j.quascirev.2014.01.003.

References

Allen, C., 1957. San Andreas fault zone in San Gorgonio Pass, southern California. Geol. Soc. Am. Bull. 68, 315–350.
Anderson, R.S., Repka, J.L., Dick, G.S., 1996. Dating depositional surfaces using in situ produced cosmogenic radionuclides. Geology 24, 47–51.
Arboleya, M.-L., Babault, J., Owen, L.A., Teixell, A., Finkel, R.C., 2008. Timing and nature of fluvial incision in the Ouarzazate foreland basin, Morocco. J. Geol. Soc. Lond. 165, 1059–1073.
Armstrong, P., Perez, R., Owen, L.A., Finkel, R.C., 2010. Timing and controls on late Quaternary landscape development along the eastern Sierra el Mayor, northern Baja California, Mexico. Geomorphology 114, 415–430.
Balco, G., Stone, J.O., Lifton, N.A., Dunai, T.J., 2008. A complete and easily accessible means of calculating surface exposure ages or erosion rates from ^{10}Be and ^{26}Al measurements. Quat. Geochronol. 8, 174–195.
Barnard, P.L., Owen, L.A., Finkel, R.C., 2006. Quaternary fans and terraces in the Khumbu Himalaya, south of Mt. Everest: their characteristics, age and formation. J. Geol. Soc. Lond. 163, 383–400.
Beaty, C.B., 1970. Age and estimated rate of accumulation of an alluvial fan, White Mountains, California, USA. Am. J. Sci. 268, 50–70.
Beaty, C.B., 1990. Anatomy of a White Mountains debris-flow—the making of an alluvial fan. In: Rachoki, A.H., Church, M. (Eds.), Alluvial Fans: a Field Approach. Wiley, Chichester, pp. 69–89.
Behr, W.M., Rood, D.H., Fletcher, K.E., Guzman, N., Finkel, R., Hanks, T.C., Hudnut, K.W., Kendrick, K.J., Platt, J.P., Sharp, W.D., Weldon, R.J., Yule, J.D., 2010. Uncertainties in slip-rate estimates for the Mission Creek strand of the southern San Andreas fault at Biskra Palms Oasis, Southern California. Geol. Soc. Am. Bull. 122, 1360–1377.
Benn, D.I., Owen, L.A., Finkel, R.C., Clemmens, S., 2006. Pleistocene lake outburst floods and fan formation along the Eastern Sierra Nevada: Implications for the interpretation of intermontane Lacustrine Records. Quat. Sci. Rev. 25, 2,729–2,748.
Bierman, P.R., Gillespie, A.R., Caffee, M.W., 1995. Cosmogenic ages for earthquake recurrence intervals and debris flow fan deposition, Owens Valley, California. Science 270, 447–450.
Bischoff, J.L., Cummins, K., 2001. Wisconsin glaciation of the Sierra Nevada (79,000–15,000 yr BP) as recorded by rock flour in sediments of Owens Lake, California. Quat. Res. 55, 14–24.
Blisniuk, K., Rockwell, T., Owen, L.A., Oskin, M., Lipponett, C., Caffee, M.C., Dortch, J., 2010. Late Quaternary slip rate gradient defined using high-resolution topography and ^{10}Be dating of offset landforms on the southern San Jacinto Fault zone, California. J. Geophys. Res. 115, B08401.
Blisniuk, K., Oskin, M., Fletcher, K., Rockwell, T., Sharp, W., 2012. Assessing the reliability of U-Series and ^{10}Be dating techniques on alluvial fans in the Anza Borrego Desert, California. Quat. Geochronol. 13, 26–41.
Blythe, A.E., Burbank, D.W., Farley, K.A., Fielding, E.J., 2000. Structural and topographic evolution of the central Transverse Ranges, California, from apatite fission-track, (U–Th)/He and digital elevation model analyses. Basin Res. 12, 97–114.
Bowman, D., 1978. Determination of intersection points within a telescopic alluvial fan complex. Earth Surf. Process. 3, 265–276.
Bull, W.B., 1977. The alluvial-fan environment. Prog. Phys. Geogr. 1, 222–270.
Bull, W.B., 1991. Geomorphic Responses to Climate Change. Oxford University Press, New York.
Bull, W.B., 2000. Correlation of fluvial aggradation events to times of global climate change. In: Noller, J.S., Sowers, J.M., Lettis, W.R. (Eds.), Quaternary Geochronology: Methods and Applications. American Geophysical Union, Washington, D.C., pp. 456–464.
Bull, W.B., 2007. Tectonic Geomorphology of Mountains: a New Approach to Paleoseismology. Blackwell Publishing, p. 328.
Cohen, K.M., Gibbard, P.L., 2011. Regional Chronostratigraphical Correlation Table for the Last 270,000 Years: Europe North of the Mediterranean. International Commission on Stratigraphy. http://www.stratigraphy.org/column.php?id=Chart/Time%20Scale (accessed October 2012).

Desilets, D., Zreda, M., 2003. Spatial and temporal distribution of secondary cosmic-ray nucleon intensities and applications to in situ cosmogenic dating. Earth Planet. Sci. Lett. 206, 21–42.

Desilets, D., Zreda, M., Prabu, T., 2006. Extended scaling factors for in situ cosmogenic nuclides: new measurements at low latitude. Earth Planet. Sci. Lett. 246, 265–276.

Duhnforth, M., Densmore, A.L., Ivy-Ochs, S., Allen, P.A., Kubik, P.W., 2007. Timing and patterns of debris flow deposition on Shepherd and Symmes creek fans, Owens Valley, California, deduced from cosmogenic ^{10}Be. J. Geophys. Res. 112, F03S15.

Dunai, T.J., 2001. Scaling factors for production rates of in situ produced cosmogenic nuclides: a critical reevaluation. Earth Planet. Sci. Lett. 176, 157–169.

Enzel, Y., Wells, S., Lancaster, N. (Eds.), 2003. Paleoenvironment and Paleohydrology of the Mojave and Southern Great Basin Deserts. Geological Society of America Special Paper, vol. 368, p. 249.

Fletcher, K.E.K., Sharp, W.D., Kendrick, K.J., Behr, W.M., Hudnut, K.W., Hanks, T.C., 2010. ^{230}Th/U dating of a late Pleistocene alluvial fan along the southern San Andreas fault. Geol. Soc. Am. Bull. 122, 1347–1359.

Frankel, K.L., Brantley, K.S., Dolan, J.F., Finkel, R.C., Klinger, R.E., Knott, J.R., Machette, M.N., Owen, L.A., Phillips, F.M., Slate, J.L., Wenicke, B.P., 2007a. Cosmogenic ^{10}Be and ^{36}Cl geochronology of offset alluvial fans along the northern Death Valley fault zone: Implications for transient strain in the eastern California shear zone. J. Geophys. Res. Solid Earth 112, B06407. http://dx.doi.org/10.1029/2006JB004350.

Frankel, K.L., Dolan, J.F., Finkel, R.C., Owen, L.A., Hoeft, J.S., 2007b. Spatial variations in slip rate along the Death Valley-Fish Lake Valley fault system determined from LiDAR topographic data and cosmogenic ^{10}Be geochronology. Geophys. Res. Lett. 34, LI8303.

Frankel, K.L., Dolan, J.F., Owen, L.A., Ganev, P., Finkel, R.C., 2011. Spatial and temporal constancy of seismic strain release along an evolving segment of the Pacific-North America plate boundary. Earth Planet. Sci. Lett. 304, 565–576.

Ganev, P.N., Dolan, J.F., Frankel, K.L., Finkel, R.C., 2010. Rates of extension along the Fish Lake Valley fault and transtensional deformation in the Eastern California shear zone-Walker Lane belt. Lithosphere 2, 33–49.

Gillespie, A.R., Clark, D.H., 2011. Glaciations of the Sierra Nevada, California, USA. In: Elhers, J., Gibbard, P., Hughes, P.D. (Eds.), Quaternary Glaciations – Extent and Chronology: a Closer Look, Developments in Quaternary Science, second ed., vol. 15. Elsevier, Amsterdam, pp. 447–462.

Hancock, G., Anderson, R., Chadwick, O., Finkel, R., 1999. Dating fluvial terraces with ^{10}Be and ^{26}Al profiles: application to the Wind River, Wyoming. Geomorphology 27, 41–60.

Harvey, A.M., 1990. Factors influencing Quaternary alluvial fan development in southeast Spain. In: Rachoki, A.H., Church, M. (Eds.), Alluvial Fans: a Field Approach. Wiley, Chichester, pp. 247–269.

Harvey, A.M., 1997. The occurrence and role of arid zone alluvial fans. In: Thomas, D.S.G. (Ed.), Arid Zone Geomorphology. Belhaven Press, London, pp. 231–259.

Harvey, A.M., Wells, S.G., 2003. Late Quatrernary variations in alluvial fan sedimentologic and geomorphic processes, Soda Lake basin, eastern Mojave Desert. In: Enzel, Y., Wells, S.G., Lancaster, N. (Eds.), Paleoenvironments and Paleohydrology of the Mojave and Southern Great Basin Deserts, Geological Society of America Special Paper 368, Boulder, Colorado, pp. 189–205.

Harvey, A.M., Silva, P.G., Mather, A.E., Goy, J.L., Stokes, M., Zazo, C., 1999a. The impact of Quaternary sea-level and climatic change on coastal alluvial fans in the Cabo de Gata ranges, southeast Spain. Geomorphology 28, 1–22.

Harvey, A.M., Wigand, P.E., Wells, S.G., 1999b. Response of alluvial fan systems to the late Pleistocene to Holocene climatic transition: contrasts between the margins of pluvial Lakes Lahontan and Mojave, Nevada and California, USA. Catena 36, 255–281.

Hedrick, K., Owen, L.A., Rockwell, T.K., Meigs, A., Costa, C., Caffee, M.W., Masana, E., Ahumada, E., 2013. Timing and nature of alluvial fan and strath terrace formation in the Eastern Precordillera of Argentina. Quat. Sci. Rev. 80, 143–168.

Hereford, R., Webb, R.H., 2002. Climate Variation since 1900 in the Mojave Desert Region Affects Geomorphic Processes and Raises Issues for Land Management (Online) Available from: http://wrgis.wr.usgs.gov/MojaveEco/Papers/climate-variation.pdf (accessed 14.08.02.).

Hidy, A.J., Gosse, J.C., Pederson, J.L., Mattern, J.P., Finkel, R.C., 2010. A geologically constrained Monte Carlo approach to modeling exposure ages from profiles of cosmogenic nuclides: an example from Lees Ferry, Arizona. Geochem. Geophys. Geosys. 11, 18. http://dx.doi.org/10.1029/2010GC003084.

Hunning, J.R., 1978. A Characterization of the Climate of the California Desert. Bureau of Land Management, Riverside, California. Contract No. CA-060-CT7-2812.

Klinger, R.E., 2001a. Late Quaternary volcanism of Ubehebe crater. In: Machette, M.N., Johnson, M.L., Slate, J.L. (Eds.), Quaternary and Late Pliocene Geology of the Death Valley Region: Recent Observations on Tectonics, Stratigraphy and Lake Cycles, Guidebook for the 2001 Pacific Cell – Friends of the Pleistocene Fieldtrip. U.S. Geological Survey, Denver, CO, pp. 21–24.

Klinger, R.E., 2001b. Road log for day A, northern Death Valley. In: Machette, M.N., Johnson, M.L., Slate, J.L. (Eds.), Quaternary and Late Pliocene Geology of the Death Valley Region: Recent Observations on Tectonics, Stratigraphy, and Lake Cycles, Guidebook for the 2001 Pacific Cell — Friends of the Pleistocene Fieldtrip. U.S. Geological Survey, Denver, CO, pp. 6–20.

Kohl, C.P., Nishiizumi, K., 1992. Chemical isolation of quartz for measurement of in-situ produced cosmogenic nuclides. Geochim. Cosmochim. Acta 56, 3583–3587.

Ku, T.L., Bull, W.B., Freeman, S.T., Knauss, K.G., 1979. ^{230}Th-^{234}U dating of pedogenic carbonates in gravelly desert soils of Vidal Valley, southeastern California. Geol. Soc. Am. Bull. Part 1 90, 1063–1073.

Lal, D., 1991. Cosmic ray labelling of erosion surfaces: in situ nuclide production rates and erosion models. Earth Planet. Sci. Lett. 104, 424–439.

Le, K., Lee, J., Lewis, A.O., Finkel, R.C., 2007. Late Quaternary slip rates along the Sierra Nevada frontal fault zone, California: slip partitioning across the western margin of the Eastern California Shear Zone/Basin and Range Province. Geol. Soc. Am. Bull. 119, 240–256.

Lecce, S.A., 1990. The alluvial fan problem. In: Rachoki, A.H., Church, M. (Eds.), Alluvial Fans: a Field Approach. Wiley, Chichester, pp. 3–24.

Lifton, N.A., Bieber, J.W., Clem, J.M., Duldig, M.L., Evenson, P., Humble, J.E., Pyle, R., 2005. Addressing solar modulation and long-term uncertainties in scaling secondary cosmic rays for in situ cosmogenic nuclide applications. Earth Planet. Sci. Lett. 239, 140–161.

Lifton, N.A., Jull, A.J.T., Quade, J., 2001. A new extraction technique and production rate estimate for in situ cosmogenic ^{14}C in quartz. Geochim. Cosmochim. Acta 65, 1953–1969.

Lowell, T.V., 1995. The application of radiocarbon age estimates to the dating of glacial sequences: an example from the Miami sublobe, Ohio, USA. Quat. Sci. Rev. 14, 85–99.

Lustig, L.K., 1965. Clastic Sedimentation in Deep Springs Valley, California. In: U.S. Geological Survey Professional Paper 352-F, pp. 131–192.

Luyendyk, B.P., 1991. A model for Neogene crustal rotations, transtension, and transpression in southern California. Geol. Soc. Am. Bull. 103, 1528–1536.

Machette, M.N., 1985. Calcic Soils of Southwestern United States. In: Geological Society of America Special Paper 203, pp. 1–21.

Machette, M.N., Slate, J.L., Phillips, F.M., 2008. Terrestrial Cosmogenic-nuclide Dating of Alluvial Fans in Death Valley, California. In: USGS Professional Paper 1755.

Martinson, D.G., Pisias, N.G., Hays, J.D., Imbrie, J., Moore, T.C., Shackleton, N.J., 1987. Age dating and the orbital theory of ice ages: development of a high resolution 0 to 300,000-year chronology. Quat. Res. 27, 1–29.

Matmon, A., Nichols, K., Finkel, R., 2006. Isotopic insights into smoothening of abandoned fan surfaces, Southern California. Quat. Res. 66, 109–118.

Matmon, A., Schwartz, D., Finkel, R., Clemmens, S., Hanks, T., 2005. Dating offset fans along the Mojave section of the San Andreas Fault using cosmogenic ^{26}Al and ^{10}Be. Geol. Soc. Am. Bull. 117, 795–807.

Matti, J., Morton, D., 1993. Paleogeographic Evolution of the San Andreas Fault in Southern California: a Reconstruction Based on a New Cross-fault Correlation. In: Geological Society of America Memoir, vol. 178, pp. 107–159.

Matti, J., Morton, D., Cox, B., 1985. Distribution and Geologic Relations of Fault Systems in the Vicinity of the Central Transverse Ranges, Southern California. U.S. Geological Survey Open File Report 85-365, scale 1:25, 0000. U.S. Geol. Survey, Reston, Virginia, p. 27.

Matti, J.C., Morton, D.M., Cox, B.F., 1992a. The San Andreas Fault System in the Vicinity of the Central Transverse Ranges Province, Southern California. USGS Open-file report, pp. 92–354.

Matti, J.C., Morton, D.M., Cox, B.F., 1992b. Distribution and Geologic Relations of Fault Systems in the Vicinity of the Central Transverse Ranges, Southern California. Unpublished map sheet 1 of 2. USGS Open-File report, pp. 92–354.

McDonald, E.V., McFadden, L.D., Wells, S.G., 2003. Regional response of alluvial fans to the Pleistocene to Holocene climatic transition, Mojave Desert, California. In: Enzel, Y., Wells, S.G., Lancaster, N. (Eds.), Paleoenvironments and Paleohydrology of the Mojave and Southern Great Basin Deserts, Geological Society of America Special Paper 368, Boulder, Colorado, pp. 189–205.

McFadden, L.D., 1982. The Impacts of Temporal and Spatial Climatic Changes on Alluvial Soils Genesis in Southern California (Ph.D). University of Arizona, p. 430.

McGill, S.F., Owen, L.A., Weldon, R.J., Kendrick, K.J., 2013. Latest Pleistocene and Holocene slip rate for the San Bernardino strand of the San Andreas fault, Plunge Creek, Southern California: implications for strain partitioning within the southern San Andreas Fault Zone for the last ∼35 k.y. Geol. Soc. Am. Bull. 125, 48–72.

Miller, D., Schmidt, K.M., Mahan, S.A., McGeehin, J.P., Owen, L.A., Barron, J.A., Lehmkuhl, F., Löhrer, R., 2010. Holocene landscape response to seasonality of storms in the Mojave Desert. Quat. Int. 215, 45–61.

Minnich, R.A., 1986. Snow levels and amounts in the mountains of southern California. J. Hydrol. 86, 37–58.

Minnich, R.A., 1984. Snow drifting and timberline dynamics on Mount San Gorgonio, California, USA. Arct. Alp. Res. 16, 395–412.

Morton, D.M., Miller, F.K., 2003. Preliminary Geologic Map of the San Bernardino 30′ x 60′ Quadrangle, California. USGS Open-File Report 03-293. http://pubs.usgs.gov/of/2003/03-293/.

Orozco, A., 2004. Offset of a Mid-Holocene Alluvial Fan Near Banning, CA; Constraints on the Slip Rate of the San Bernardino Strand of the San Andreas Fault (M.S. thesis). California State University at Northridge, Northridge, California, p. 56.

Orozco, A., Yule, D., 2003. Late Holocene slip rate for the San Bernardino strand of the San Andreas fault near Banning, California. Seismol. Res. Lett. 74, 237.

Owen, L.A., Windley, B.F., Cunningham, W.D., Badamgarov, G., Dorjnamjaa, D., 1997. Quaternary alluvial fans in the Gobi Desert, southern Mongolia: evidence for neotectonics and climate change. J. Quat. Sci. 12, 239–252.

Owen, L.A., Finkel, R.C., Minnich, R., Perez, A., 2003. Extreme southern margin of Late Quaternary glaciation in North America: timing and controls. Geology 31, 729–732.

Owen, L.A.., Finkel, R.C., Ma, H., Barnard, P.L., 2006. Late Quaternary landscape evolution in the Kunlun Mountains and Qaidam Basin, Northern Tibet: a framework for examining the links between glaciation, lake level changes and alluvial fan formation. Quat. Int. 154–155, 73–86.
Owen, L.A., Frankel, K.L., Knott, J.R., Reynhout, S., Finkel, R.C., Dolan, J.F., Lee, J., 2011. Beryllium-10 terrestrial cosmogenic nuclide surface exposure dating of Quaternary landforms in Death Valley. Geomorphology 125, 541–557.
Ponti, D.J., 1985. The Quaternary Alluvial Sequence of the Antelope Valley, California. In: Geological Society of America Special Paper 203, pp. 79–96.
Quigley, M.C., Sandiford, M., Cupper, M.L., 2007. Distinguishing tectonic from climatic controls on range-front sedimentation. Basin Res. 19, 491–505.
Rawson, P.F., Allen, P.M., Brenchley, P.J., Cope, J.C.W., Gale, A.S., Evans, J.A., Gibbard, P.L., Gregory, F.J., Hailwood, E.A., Hesselbo, S.P., Knox, R.W.O.'B., Marshall, J.E.A., Oates, M., Riley, N.J., Smith, A.G., Trevin, N., Zalasiewicz, J.A., 2002. Stratigraphic Procedure. Geological Society Professional Handbook, London, p. 57.
Reheis, M.C., Slate, J.L., Throckmorton, C.K., McGeehin, J.P., Sarna-Wojcicki, Dengler, L., 1996. Late Quaternary sedimentation on the Leidy Creek fan, Nevada-California: geomorphic responses to climate change. Basin Res. 12, 279–299.
Ritter, J.B., Miller, J.R., Enzel, Y., Wells, S.G., 1995. Reconciling the roles of tectonism and climate in Quaternary alluvial fan evolution. Geology 23, 245–248.
Rockwell, T.K., Keller, E.A., Johnson, D.L., 1985. Tectonic geomorphology of alluvial fans and mountain fronts near Ventura, California. In: Morisawa, M., Hack, J.T. (Eds.), Tectonic Geomorphology. Allen and Unwin, London, pp. 183–209.
Rosholt, J.N., Bush, C.A., Carr, W.J., Hoover, D.L., Swadley, W.C., Dooley Jr., J.R., 1985. Uranium-Trend Dating of Quaternary Deposits in the Nevada Test Site Area, Nevada and California. USGS Open-File Report, pp. 85–540.
Salton Sea Authority, 2002. Geography of the Salton Sea (Online) Available at: http://saltonsea.ca.gov/geography.htm (accessed 14.08.02.).
Sharp, R.P., Allen, C.R., Meier, M.F., 1959. Pleistocene glaciers on southern California Mountains. Am. J. Sci. 257, 81–94.
Sohn, M.F., Mahan, S.A., Knott, J.R., Bowman, D.D., 2007. Luminescence ages for alluvial-fan deposits in Southern Death Valley: implications for climate-driven sedimentation along a tectonically active mountain front. Quat. Int. 166, 49–60.
Sowers, J.M., Amundson, R.G., Chadwick, O.A., Harden, J.W., Jull, A.J.T., Ku, T.L., McFadden, L.D., Reheis, M.C., Taylor, E.M., Szabo, B.J., 1989. Geomorphology and pedology on the Kyle Canyon alluvial fan, southern Nevada. In: Rice Jr., T.J. (Ed.), Soils Geomorphology Relationships in the Mojave Desert, California, Nevada: Field Tour Guidebook for the 1989, Soil Science Society of America Annual Meeting Pre-Meeting Tour, October 12–14, 1989, pp. 93–112.
Spelz, R.M., Fletcher, J.M., Owen, L.A., Caffee, M.W., 2008. Quaternary alluvial-fan development, climate and morphologic dating of faults scarps in Laguna Salada, Baja California, Mexico. Geomorphology 102, 578–594.
Stokes, M., Nash, D.J., Harvey, A.M., 2007. Calcrete 'fossilisation' of alluvial fans in SE Spain: the roles of groundwater, pedogenic processes and fan dynamics in calcrete development. Geomorphology 85, 63–84.
Stokes, S., Kocurek, G., Pye, K., Winspear, N.R., 1997. New evidence for the timing of Aeolian sand supply to the Algodones dunefield and east Mesa area, southeastern California, USA. Palaeogeogr. Palaeoclimatol. Palaeoecol. 128, 63–75.
Stone, J.O., 2000. Air pressure and cosmogenic isotope production. J. Geophys. Res. 105, 753–759.
Van Devender, T.R., 1990. Late Quaternary vegetation and climate of the Sonoran Desert, United States and Mexico. In: Betancourt, J.L., et al. (Eds.), Packrat Middens: the Last 40,000 Years of Biotic Change. University of Arizona Press, Tucson, pp. 134–165.
van der Woerd, J., Klinger, Y., Sieh, K., Tapponnier, P., Ryerson, F.J., Meriaux, A., 2006. Long-term slip rate of the southern San Andreas fault from ^{10}Be-^{26}Al surface exposure dating of an offset alluvial fan. J. Geophys. Res. 111, B04407. http://dx.doi.org/10.1029/2004JB003559, 17 pp.
Weldon, R.J., Sieh, K.E., 1985. Holocene rate of slip and tentative recurrence interval for large earthquakes on the San Andreas fault in Cajon Pass, southern California. Geol. Soc. Am. Bull. 96, 793–812.
Wells, S.G., McFadden, L.D., Dohrenwend, J.C., 1987. Influence of late Quaternary climatic changes on geomorphic and pedogenic processes on a desert piedmont, eastern Mojave Desert, California. Quat. Res. 27, 130–146.
Wells, S.G., McFadden, L.D., Harden, J., 1990. Preliminary results of age estimations and regional correlations of Quaternary alluvial fans within the Mojave Desert of Southern California. In: Reynolds, R.E., Wells, S.G., Brady, R.J.I. (Eds.), At the End of the Mojave: Quaternary Studies in the Eastern Mojave Desert. Special Publications of the San Bernardino County Museum Association, Redlands, CA, pp. 45–53.
Yule, D., Sieh, K., 2003. Complexities of the San Andreas fault near San Gorgonio Pass: implications for large earthquakes. J. Geophys. Res. 108 (B11), 2548. http://dx.doi.org/10.1029/2001JB000451.
Yule, D., 2009. The enigmatic San Gorgonio Pass. Geology 37, 191–192.
Yule, D., Spotila, J., 2010. Quaternary geology of the San Bernardino Mountains and their tectonic margins. In: Clifton, E.H., Ingersoll, R.V. (Eds.), Geologic Excursions in California and Nevada: Tectonics, Stratigraphy and Hydrogeology. Pacific Section SEPM (Society for Sedimentary Geology), Upland, California, pp. 273–322. Book 108.
Yule, D., Fumal, T., McGill, S., Seitz, G., 2001. Active tectonics and paleoseismic record of the San Andreas fault, Wrightwood to Indio: working toward a forecast for the next "Big Event,". In: Dunne, G., Cooper, J. (Eds.), Geologic Excursions in the California Deserts and Adjacent Transverse Ranges, Fieldtrip Guidebook and Volume Prepared for the Joint Meeting of the Cordilleran Section Geological Society of America and the Pacific Section American Association of Petroleum Geologists, 9–11 April 2001. Pacific Section SEPM (Society for Sedimentary Geology), Universal City, California, pp. 91–126.
Zehfuss, P.H., Bierman, P.R., Gillespie, A.R., Burke, R.M., Caffee, M.W., 2001. Slip rates on the Fish Springs fault, Owens Valley, California, deduced from cosmogenic ^{10}Be and ^{26}Al and soil development on fan surfaces. Geol. Soc. Am. Bull. 113, 241–255.